The Specialist Committee on Azimuthing Podded Propulsion

Final Report and Recommendations to the 25th ITTC

1 MEMBERSHIP AND MEETINGS

1.1 Membership

The 24th ITTC appointed the Specialist Committee on Azimuthing Podded Propulsion with the following membership:

- Dr. Noriyuki Sasaki (Chairman).
  National Maritime Research Institute (NMRI), Tokyo, Japan.
- Ir. Jaap H. Allema.
  Maritime Research Institute Netherlands (MARIN), Wageningen, The Netherlands.
- Professor Mehmet Atlar.
  University of Newcastle, Newcastle-upon-Tyne, United Kingdom.
- Dr. Se-Eun Kim.
  Samsung Heavy Industries Co. Ltd., Taejeon, Korea.
- Dr.Valery Borusevich.
  Krylov Shipbuilding Research Institute (KSRI), St. Petersburg, Russia.
- Dr. Antonio Sanchez-Caja.
  VTT Industrial Systems, Espoo, Finland.
- Dr. Francesco Salvatore.
  Istituto Nazionale per Studi ed Esperienze di Architettura Navale (INSEAN), Roma, Italy.
- Professor Chen-Jun Yang (Secretary).
  Shanghai Jiao Tong University (SJTU), Shanghai, China.

1.2 Meetings

At the first meeting of the Committee, Professor Chen-Jun Yang was elected as Secretary of the Committee. Four formal meetings of the Committee were held as follows:

- Tokyo, Japan, March 2006.
- Brest, France, October 2006, in conjunction with the 2nd T-Pod Conference.
- St. Petersburg, Russia, June 2007.
- Shanghai, China, March 2008.

2 RECOMMENDATIONS OF THE 24TH ITTC (*COMMITTEE'S TASKS*)

1. Review and update Procedure 7.5-02-03-01.3 "Propulsion, Performance-Podded Propulsor Tests and Extrapolation". Give special emphasis on how to scale housing drag and to the validation of full-scale propulsion prediction.

2. Continue the review of hydrodynamics of POD propulsion for special applications including fast ships, ice going ships (Liaise with the Ice committee) and special POD arrangements like Contrarotating Propellers (CRP) and hybrids. Include the practical application of computational methods to prediction and scaling.

3. Review and analyse the cavitation behaviour of podded propulsors. Emphasize high pod angles and normal steering angles including dynamic behaviour. Include the practical application of computational methods to prediction and scaling.

3 INTRODUCTION

3.1 General Remarks

It is very obvious that the technology of Podded Propulsion tests have much progressed in the field of not only simple application as propulsion system for conventional vessel such as cruise ships but also complex application such as double action ships (DAS) and hybrid contra rotating podded propulsion installed on high speed RO/RO vessel (HAMANASU). Another remarkable change is the increment of application of podded propulsion system of smaller size.

Fast Ship Application for Pod Drives (FASTPOD) was a collaborative Research and & Technical Development (RTD) project participated by 17 partners from 7 European countries. The project ran three years between 2002 and 2005 and was sponsored by the European Commission through the Fifth Framework Program (FP5). The principal objective of the FASTPOD project was to explore a new design technology to exploit the benefit that can be offered when using electric pod drives on commercial large and fast ships (35-40kts) in an efficient, safe and environmental friendly manner.

SES (Super Eco-Ship) projects in Japan has been promoting many novel coastal ships driven by podded propulsion system. The projects started from 2001 and can be divided into two projects. SES phase1 is a project for developing new technology concerned with electric propulsion system including podded propulsor and the research programme was finalised in 2005 and the project has established economical supporting system of new buildings of novel ships with electric driven propulsor. The second project is called SES phase 2 and the project aims to develop combined system of marine gas turbine and pure CRP podded propulsor. The first vessel of SES phase 1 “Shin-ei Maru” was delivered 2007 and the first vessel of SES phase 2 “Shige Maru”was 2008.

3.2 Report layout

From herein, the report content is as follows:

- Section 4: State-of-the-art review
- Section 5: Podded propulsor tests and extrapolations (*Task 1*)
- Section 6: Guidelines on extrapolation to full-scale (*Task 1*)
- Section 7: Questionnaire
- Section 8: Dynamic behaviour at high pod angles (*Task 3*)
- Section 9: Special applications for podded propulsion (*Task 2*)
- Section 10: Technical conclusions
- Section 11: References
- Appendix A: Improved interim procedures (7.5-02-03-01.3) for podded propulsor tests and extrapolation

4 STATE-OF-THE-ART

4.1 Introduction

The following is an update on some high-profile pod related R&D activities, interesting landmark applications of pod driven ships, dedicated international conferences and other related events to reflect on the state-of-the-art on pod propulsion since the 24th ITTC reporting.

4.2 Research and development activities

In Europe, under the EC Framework Programme (FP5), a 3 year RTD project FASTPOD (Fast Ship Applications of for Pod Drives) participated by 17 EU partners from 7 EU countries was completed in early 2006. The principle objective of the FASTPOD project was to explore a new design technology to exploit the benefits that can be offered when using electric pod drives on commercial large and fast ships (35-40 knots) in an efficient, safe and environmentally friendly manner. The project explored the potential applications of conventional pod motor technology on a conventional ropax (38 knots) and container ship (35 knots) as well as a trimaran cargo vessel (40 knots) using numerical and experimental methods. An overall summary and conclusions of this project is given by

Atlar et al. (2006) including a list of publications generated by the project.

In parallel with FASTPOD, other FP5 project conducted was the combined R&D and Technology Platform VRSHIPS-ROPAX 2000 (Life-Cycle Virtual Reality Ship Systems), **VRSHIPS-Ropax, (2006)**. This four years research programme with more than 30 partners was also completed in 2006 and had the objectives of implementing, developing and realising an independent, generic, integrated platform for virtual modelling and simulation of critical marine technologies and to realise an application of this platform by targeting the design of an advanced ropax concept. With this objective, in collaboration with FASTPOD, the project partners demonstrated that it was viable to drive a fast ropax using an innovative hybrid propulsion system including twin steerable pods and twin fixed water jets as discussed in Section 9.5.

In 2005 a long term research programme has been initiated by the Italian Ship Model Basin (INSEAN) with the aim of developing theoretical and experimental tools that may be used to investigate hydrodynamics and hydro-acoustics of podded propulsor. The first phase of this programme involved the validation of and existing single propeller simulation code and its extension to the analysis of complex multi-component configurations with rotating and fixed parts in unsteady cavitating flow using boundary element methods as reported in **Greco et al. (2006).** In parallel, propeller-strut interactional aspects were investigated through Laser Doppler Velocimetry techniques and high-speed video extending a methodology used to analyse propeller-rudder phenomena **(Felli et al, 2006).** Podded ship performance and manoeuvrability tests are scheduled in 2008-09 to compare performances of conventional propellers and pod propulsion with reference to an existing twin-screw navy supply vessel.

A four-year R&D project was started in 2006 at SVA (Potsdam, Germany) on innovative high-efficiency pods based on the High Temperature Superconductor (HTS) technology. Objective of the project is to investigate the feasibility of electric ship propulsion based on this innovative technology. Reducing weight and volume of standard electrical equipment in copper, HTS materials can allow for dramatic increase in motor power density and power throughput. This technology can be exploited to develop innovative pod systems with gondola diameters 40% smaller than existing solutions, with inherent advantages in terms of efficiency and reduced noise and vibration excitations. The impact of this new technology on podded propulsors is studied in this R&D project by SVA. Design and optimisation of a vessel adopting podded drives based on the HTS technology is addressed. Experimental investigations are planned to determine performance of these pods including cavitation properties and off-design conditions.

Another EU initiative, under FP6 and involving pod related research, is the five years (2006- 2011) European Network of Excellence (NoE) project HTA (An alliance to enhance the maritime testing infrastructure in the EU). The main objective of this network is to develop a formal and lasting structure to co-ordinate the definition and introduction of novel measurement, observation and analyses technologies for hydrodynamic (scale) model testing environments. The alliance has 18 members from 10 EU countries including the leading hydrodynamic testing facilities and universities as reported in **HTA (2006)**. The main research work in the NoE is carried out by the nine Joint Research Programmes (JRP) involving specific areas of research and amongst them JRP4 (Pod/Dynamics forces) is related to pod research with the main objectives of improving model testing techniques for: the pod global and local force measurements; minimising pod model motor size; model-full scale correlations of hydrodynamic forces on a pod unit.

In a PhD thesis **Oosterhuis (2006)** designed and implemented a prototype model pod propulsor. This is directly driven by its electric motor inside the pod housing similar to a full-scale pod, and hence providing obvious superiority over the current model pod propulsors that are driven by external motors in

combination with bevel gear systems that introduce undesirable limitations and other effect. In the thesis 3 different design solutions, which are based on electrical and hydraulic motor options, were proposed and two of them using enhanced power density of electric motors were implemented in dry and wet conditions in combination with a new 6 component balance. The measurement of the propeller and pod-unit loads on the new and conventional pod/balance system, which were fitted side by side on the same hull model, clearly indicates the advantage of the new system in terms of improved accuracy, vibrations and resonant frequencies

Through another ongoing PhD research, a very different topic related to pod design was tackled by a joint collaborative effort between University of Newcastle and Sumitomo Heavy Industries Ltd in addressing concerns of cavitation during propeller ice interaction. An ongoing experimental research program introduced innovative and novel propeller ice interaction tests in a cavitation tunnel to systematically study the phenomena. The objective of the research was to quantify the effect of cavitation during propeller ice interaction, something that at present, is not considered in any experimental facility. Findings so far indicate that cavitation is a significant factor leading to highly oscillatory blade loading, blade fatigue, elevated noise and possible erosion effects noted by **Sampson et al. (2006)**.

In Canada a 5 year national research programme on podded propellers was completed in 2007 and undertaken jointly by the Ocean Engineering Research Centre at Memorial University of Newfoundland, the National Research Council's Institute for Ocean Technology, Oceanic Consulting Corporation and Thordon Bearings Ltd. This research programme combined parallel developments in numerical prediction methods and experimental evaluation. The work addressed gaps in the knowledge concerning podded propeller performance, performance prediction, and performance evaluation. The short-term objectives aimed: (1) To quantify systematically the effect of podded propulsor configuration variations on propulsion performance; (2) To develop computational methods for performance prediction; (3) To develop an extrapolation method for powering prediction of ships fitted with pod driven ships; (4) To quantify the blade loading effects in open water and in ice at off-design conditions; to develop new instrumentation for performance evaluation; (5) To develop speciality manufacturing capability in Canada for high quality model propulsors. Amongst the hydrodynamic issues that were identified are questions regarding the effects of hub taper angle, pod-strut configuration, pod-strut interactions, gap pressure and pod-strut geometry on podded propeller performance. An overall review of this research programme are presented in a recent paper by **Islam et al. (2007).**

In Japan, in order to address the land bound transport problems and the emission demands of the Kyoto Protocol, a national research programme, entitled "Super Eco-Ship", has been initiated in 2001 by the Japanese Government in collaboration with the National Maritime Research Institute (NMRI) and Nakashima propeller. To promote the modal shift of cargo transportation from trucks to ships, this project aims to develop novel coastal ships driven by different pod drives (including conventional puller pod, "pure" CRP-Pod and hybrid CRP Pod) drives with higher cargo capacity, propulsive efficiency, high manoeuvrability and less vibration and noise. The R&D part of this research programme was finalised in 2005 and the project has moved on to actual building of coastal vessels driven by these pods. **Kano et al. (2006)** presents the powering and manoeuvrability characteristics of 749GT cement tanker driven by these three different type pod propulsors in comparison. From model tests and CFD works, the hybrid pod system and stern shape with stern bulb was selected from not only propulsive efficiency view point but also manoeuvrability point of view.

4.3 International conferences and other related events

T-POD 2004 (Technological Advances in Podded Propulsion) was the first international conference which was dedicated to the azimuthing podded propulsion and held in Newcastle University in association with the FASTPOD project. The theme of this conference was to discuss the past, present future of the pod propulsion over 37 technical papers was reported in **Atlar et al. (2004).**

Within the same spirit of the 1st T-POD, the second conference, T-POD 2006 was held in L'Aber Wrac'h in France and organised by Institute de Recherche de l'Ecole Navale (ENSIETA), University of Newcastle and DCN Propulsion in 3-5 October 2006. This conference was attended by over 100 delegates and 33 technical papers was presented in the fields of: Design; New concepts; Numerical hydrodynamics; Motorisation; Cavitation; Manoeuvring; Others (including seakeeping, reliability and redundancy). The conference papers are freely accessible in **Billard et al. (2006).**

Apart from the 2nd T-POD conference, since the 24th ITTC, there have been other international events where limited amount of dissemination can be found regarding to podded propulsion, e.g. in WMTC 2006, STAB'06, Propeller/Shafting'06, CAV2006, MARSIM 2006, ICETECH'06, POAC'07, OMAE'07, FAST'07, IMAM'07, ICME-ABS 2007, CMHSC 2007, ICETECH'08.

4.4 Landmark applications for podded drives

Since the last ITTC there has been a steady increase in the number of pod driven vessel applications in full-scale reflecting certain maturity of this technology. Some of these applications have been the repeat (sister ships) of the earlier designs especially in the cruise and ice-breaker market while some applications are pioneering and therefore noteworthy to report.

In Japan, 4999 DWT coastal oil tanker "Shige Maru" which is equipped with 2 x 1.25MW "pure" CRP pod to achieve a 13.5 knots service speed was delivered at Niigata Shipbuilding & Repair Inc in October 2007 and underwent extensive sea trials, as shown in Fig. 9.4. This is one of the demonstrators developed under the "Super Eco-Ship" R&D programme and the first representative of new generation environmentally friendly coastal ships.

In France, two "Mistral" class Landing Platform Dock (LPD) vessels driven by pods for the French Navy were built by the joint efforts from Chantiers de l'Atlantique and DCN and delivered in 2005 and 2006. These vessels have 21,500 tons displacement and can achieve a 19 knots max speed as well as special slow speed missions using their 2 x 7MW puller pods effectively, **Mistral (2006)**.

In arctic applications the USCGC "GLIB Mackinaw" is the first US pod driven icebreaker (cutter) built by Marinette Marine Corp. and commissioned in June 2006. The vessel has 3500 full load displacement and can achieve 15 knots using conventional 2 x 3.33MW puller pods with 4 bladed and 3.05m diameter propellers, **USCG (2008).**

Following the success of the world's pioneering double acting tanker applications, the first double acting container/cargo ship application has been the 18,000 DWT, 648TEU "MS Norilskiy Nickel" which was built by Aker Yards and delivered in mid 2006 as shown in Fig. 9.1. The propulsion is by means of a single 13MW puller pod unit with a 4 bladed propeller of 5.6m diameter, **Wilkman et al (2007).**

Increasing activities in arctic and introduction of new stake holders in the oil/gas market have not only increasing the number of the DAT driven by pods in different countries but also widening the application of this technology in other missions, for example, pioneering double acting LNG vessels.

5 PODDED PROPULSOR TESTS AND EXTRAPLOLATION

5.1 Purpose of procedures

The purpose of the procedures for podded propulsor tests and extrapolation is to describe procedures relating to azimuthing podded propulsors (or thrusters), for undertaking the following model tests and where necessary,

extrapolation to full scale. The three performance tests used are:

- Pod unit open water test
- (Self) Propulsion test

All of the above tests may not be required during a particular study of performance of a podded propulsor or in the extrapolation of model test results to full scale.

It should be noted that in this test and extrapolation procedure, the difference between a mechanical azimuthing thruster unit and an azimuthing podded propulsor is non-existent from a hydrodynamical point of view, thus both types of propulsors are from here on referred to as 'podded propulsors'. The procedure is valid for the two known variants of thrusters/podded propulsors: 'pulling' units and 'pushing' units. The maximum number of units used in the procedure is restricted to two.

The use of nozzles on podded propulsors is in development, although ducted propellers are commonly used on mechanical thrusters. The use of nozzles on electric podded propulsors is now left out of consideration in this procedure and should be treated in future ITTC work. Figure 5.1 is a simple flowchart showing the sequence and interrelation between the above tests to be able to make power prediction for a pod driven ship in full-scale.

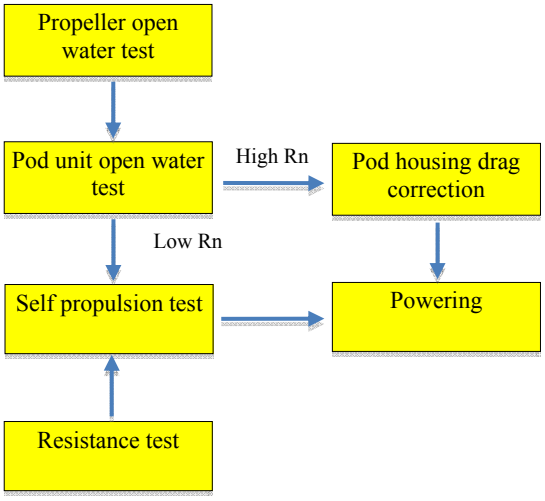

Figure 5.1: Flow diagram for full scale power prediction from model test results of a vessel equipped with podded propulsion.

The procedure for propeller open water tests for a ship equipped with podded propulsors is analogous to that of Procedure 7.5-02-03-02.1 '*Propeller open water tests*', **ITTC (2002b).**

5.2 Pod unit open water test

The pod unit open water test is a test of the complete unit with propeller and pod housing.

5.2.1 Test objectives

Pod unit open water tests have four main goals:

1. To determine the podded propulsor open water performance. This may be for full scale or for an analysis of podded propulsion tests to determine the propulsion factors for extrapolation of test results.
2. To determine data for the final propeller design from tests with stock propellers.
3. To optimize the hydrodynamic design of the podded drive units for the drive manufacturers.
4. To compare the test results with those of the propeller open water test to analyze the effect of the pod housing on the propeller open water characteristics.

5.2.2 Test conditions

The test conditions for an open water test of a podded propeller are the same as a conventional propeller. The tests should be conducted under the constant revolutions at least for two rates of rotation:

- Rpm close to the matching podded propulsor open water test for an analysis of the propeller-pod housing interaction.
- Rpm as high as possible to minimize Reynolds scale effects (laminar flow effects); this is essential for a prediction of full scale propeller performance for the propeller designer as well as for the speed-power prediction.

5.2.3 Set up

A special test set-up is required for this test. The recommended test configuration is shown in Figure 5.4, a photo of a typical set-up is shown in Figure 5.5.

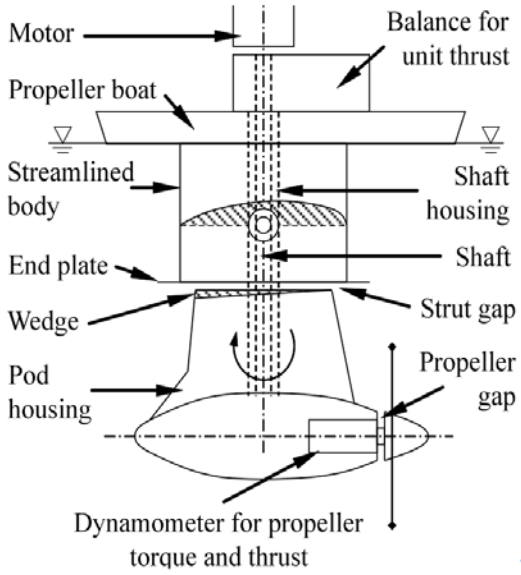

Figure 5.4: Podded propulsor in open water test setup

Figure 5.5: Typical pod unit open water test setup

In this test set-up the propeller was driven by a motor mounted on a multi-component measuring frame fitted between the top support plate (detailed in Figure 5.4) and the bottom of the propeller boat. To avoid any water surface effects, the propeller shaft must be immersed at a minimum depth of 1.5 propeller diameters (1.5D), preferably 2D. It must also be emphasized that the top of the strut should also be well submerged during the test.

(1) Shaft housing cover and end plate

The exposed part of the shaft between the top support plate and the top section of the pod strut, must be protected by means of a streamlined fairing, described as "shaft housing" in Figure 5.6, to prevent the drive shafts creating drag themselves. The fairing is carefully streamlined to the specific setup and fixed to the bottom of the top support plate.

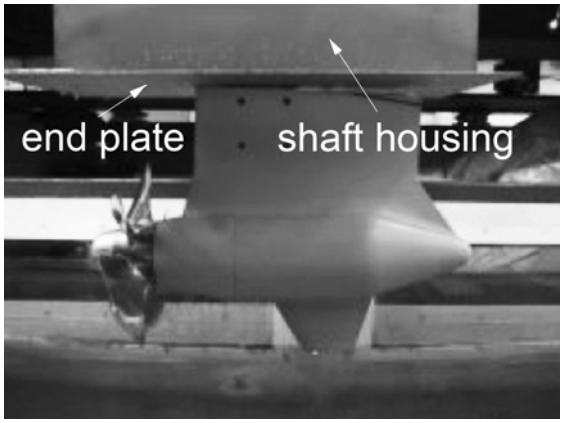

Figure 5.6: Shaft housing and end plate

A thin end plate is fitted horizontally to the bottom of the streamlined body, also shown in Figure 5.6. The plate is oversized and allowed to protrude uniformly over the fairing. The plate prevents the induction of vertical flow components due to the difference in size between streamlined body and pod strut, which could affect the flow over the pod strut.

(2) Top support plate

The top support plate is fitted to the towing carriage as close as possible to the water surface, but with a maximum allowable distance, to prevent surface wave effects.

(3) Propeller shaft line and wedge

The propeller shaft must be set horizontal to the free surface. If in this position the pod strut has an inclined top section, the top section must be made horizontal by the addition of a wedge, as shown in Figure 5.7. The inclusion of the wedge will prevent an uneven strut gap, which may affect the pod performance. This wedge will add some wetted surface to the pod, but it is expected that its effect on the pod resistance is much smaller than the effects of an inclined strut top section.

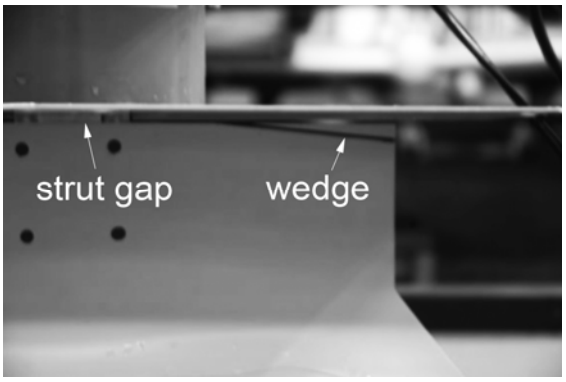

Figure 5.7: Strut gap and wedge

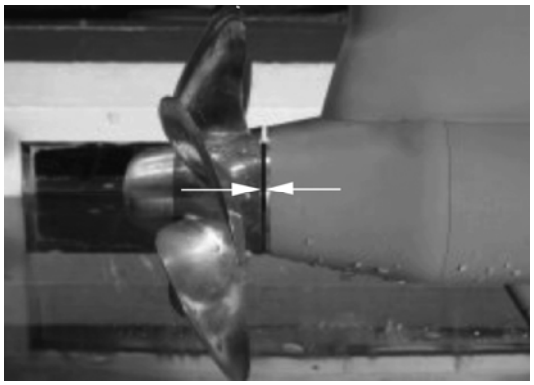
Figure 5.9: Propeller gap during experiments

(4) Strut gap

During set-up of the pod unit, there is also a gap present between strut top and the lower end-plate of the test set-up, as shown in Figure 5.7. This gap can affect pod resistance as illustrated in the results of a puller type pod resistance tests shown in Figure 5.8. The gap between the top of the strut and the end-plate should preferably be kept as small as possible, as this is not representative of the full scale condition. Nevertheless, a certain gap is required to allow some motion of the pod housing relative to the end plate.

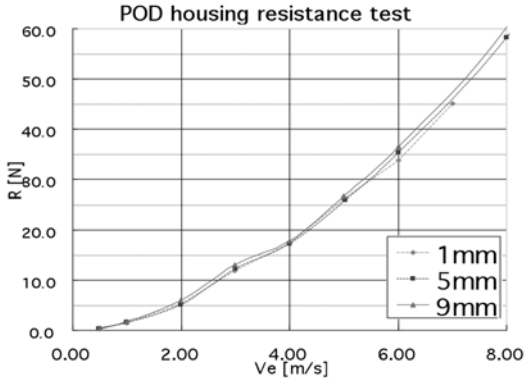

Figure 5.8: Pod resistance from Table 5.4 with different strut gaps

(5) Propeller gap

A typical view of propeller gap is shown in Figure 5.9. The width of the propeller gap has little effect on the measured pod unit thrust, but may have a significant effect on the propeller performance. In the case of thrusters or pods that have propellers with strong conical hubs such as pulling units, the propeller thrust deviates quite substantially from that of similar propellers with more cylindrical hubs.

Flow pressures in the gap cause additional forces on the propeller hub and the adjacent circular end section of the pod housing. Both forces are similar in strength but act in opposite directions, thus the propeller thrust measurement is affected, but the unit thrust measurement, containing both forces which cancel each other, is not affected.

This implies that the gap width is important, but only for the determination of the performance of the propeller on the pod. Measurements from several hydrodynamic institutes have shown that differences in propeller thrust of up to 8% between propellers with a conical hub and with a cylindrical hub. A typical example of this effect is shown in Figure 5.10 from **van Rijsbergen and Holtrop (2004)**.

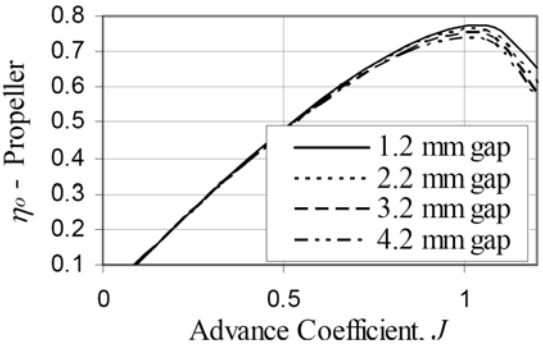

Figure 5.10: Open water efficiencies of a pod unit based on measured propeller thrust for different propeller gap widths, **van Rijsbergen and Holtrop (2004)**

One renown podded drive manufacturer specifies a maximum pod/propeller gap width on their full scale units of 10 mm, in order to avoid problems with cables and ropes getting caught in the gap and could obstruct the pods. When scaling down this gap width, it would

mean a model scale value of about 0.5 to 0.3 mm. This is not possible in model tests, which require a gap of at least 1 mm to avoid any possible interference between propeller hub and pod housing.

The recommended gap width to be applied in model tests is therefore 1mm-3mm. In particular, if a fixed aft fairing is used in the propeller open water test, it is recommended to adopt the same gap used in the propeller open water test and propulsion test to avoid uncertainty; it is not easy to analyze a gap, which includes several complex phenomena including:

- Difference of potential wake due to pod housing
- Discontinuity effect on flow around pod housing front end
- Inner pressure effect between hub and pod housing

Further investigations are necessary to understand and quantify this gap effect, as well as determining its scale effect, to be able to make correction for it in the pod open water performance. Thrust and torque of the propeller should be measured by means of a dynamometer fitted to the propeller shaft, as close as possible to the propeller, to prevent any disturbance in the measurements from mechanical friction. The pod unit thrust must be measured in the multi-component measuring frame on the top support plate.

(6) Turbulence stimulator

There are two kinds of Reynolds scale effects that must be considered during the pod unit open water tests. The first effect, which is associated with the propeller blades, can be assumed similar to that experienced in propeller open water tests. The second effect is associated with the pod housing and can be relatively large; it should be investigated before the pod unit open water test.

If resistance test of a pod unit without the effect of propeller is conducted, the use of turbulence stimulator on the pod housing is essential to improve the low Reynolds number effect involving extensive laminar flow and even flow separation on the pod. It is believed that the magnitude of the Reynolds number effects associated with the pod housing for puller pod is much smaller compared to the pusher type pod due increased turbulence caused by the propeller flow action. According to **Mewis (2001)** the Reynolds number effects on the pod housing can be neglected if the propeller Reynolds number reaches up to 5 x 10^5. Figure 5.11 shows typical arrangement of turbulence stimulators (artificial roughening) applied on the strut, pod body and fin components of a puller pod unit, indicated with arrows.

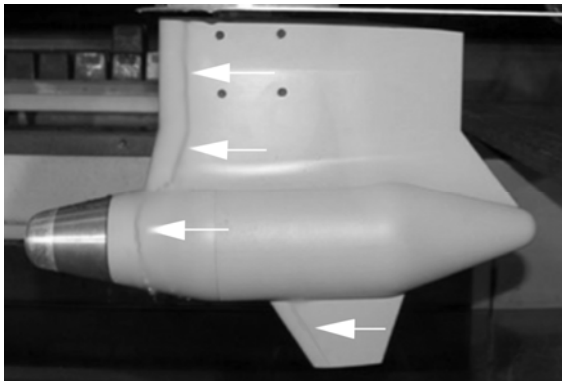

Figure 5.11: Typical turbulence stimulator arrangement applied to pod housing.

(7) Full scale correction

The podded propulsor open water test should be carried out using the same procedure as described for the propeller open water test in the previous section. The full scale correction of propeller thrust and torque coefficients should be done in the same manner as a propeller in isolation. One approach is to use the method proposed in the ITTC'78 Extrapolation Procedure. The drag of the model pod housing should be corrected according to the methods as described in Section 6.2, to arrive at the full scale unit thrust, as well as the matching full scale unit efficiency.

5.3 Self propulsion test

This is a test of the model hull fitted with complete podded propulsor(s) and driven by the propulsor(s).

5.3.1 Test objectives

Podded propulsor (self) propulsion tests are required:

1. To predict the ships calm water performance with the best possible accuracy
2. To predict the propulsor-hull interaction coefficients

5.3.2 Test conditions

After a resistance test of ship without a pod unit (same as a conventional propeller case), it is recommended that for ships fitted with podded propulsors, self-propulsion tests should be conducted with both the ship speed and the propulsor load varied independently. In addition to Skin Friction Correction of the hull surface, load correction due to pod housing drag correction (ΔK_{TU}) should be considered.

5.3.3 Test set up

The self-propulsion test should preferably be carried out in the following manner:

- The pod propellers are to be driven from the top of the unit by an electric motor, through a belt drive or a geared set of a horizontal and a vertical shafts.
- Thrust and torque of the propeller are to be measured close to the propeller. Alternatively the electrical motor could be located inside the pod for direct driving provided that the testing facility has such device available.
- The unit thrust is to be measured by means of an at least 2 component measuring frame at the intersection of the pod strut with the ship model, on which frame the motor is fitted.

Experience with pod testing has shown that a simple measurement of unit thrust by means of a longitudinal force transducer between vertical drive shaft and ship model does not work because it is affected by thrust and torque effects between motor and shaft when the motor is simply fitted to the bottom of the model. A point of special concern is air leakage from the hull along the vertical drive shaft of the pod into the water. Especially for pushing units this may occur, because of the suction effect of the working propeller that creates a low pressure area around the strut. Air leakage may lead to propeller ventilation and should thus be prevented. For instance thin flexible latex hoses can be used to close off the opening between ship model hull and the tube around the drive shaft of the thruster model.

Furthermore, care is to be taken that the Reynolds number of the flow around the pod models is high enough to avoid extensive laminar flow and even flow separation on the pod units. In general the Reynolds number must be as large as large as possible ship and pod models. The use of turbulence tripping on the pod housings helps to locally remedy a delayed flow transition, but is mostly of interest for pushing pods. The turbulent flow from the propeller will ensure in general a good enough turbulent flow over the housing of a pulling pod.

For the pod housing drag, in first instance the difference between the propeller thrust (as the propeller attached to the pod) and unit thrust can be taken. However, as explained previously, the gap between propeller hub and pod housing affects the measurement of propeller thrust. Furthermore, scale effects are present on the measured pod housing drag and they should be corrected for as described in Section 3.2. Alternatively, the pod housing drag can be obtained through pod resistance tests (pod open water tests without the propeller) and through ship model resistance tests with and without un-propelled pod model, thus viewing the pod housing as an appendage, instead as a part of the propulsor. However, this would mean that the effect of the working propeller on the pod housing resistance is neglected.

Furthermore, the thrust deduction fraction would relate the propeller thrust to the ship resistance and not the unit thrust; the wake fraction will also be different from the one determined from an open water test on the complete podded propulsion unit. The same applies to total propulsive efficiency, relative rotative efficiency, etc. In fact this alternative method is less advisable, which conclusion was already established by the Specialist Committee on Unconventional Propulsors in their Final

Report and Recommendations to the 22nd ITTC, **ITTC (1999)**, stating that for ships with for instance Z-drives, these propulsors should be tested as complete units and should not be broken down into tests on their components, being thruster/pod housing and propeller **ITTC (1999).**

In model tests in which the pod arrangement is optimized by systematically varying the longitudinal and transverse pod position, pod neutral steering angle and pod tilt angle, care should be taken to preserve the propeller tip-hull clearance. This applies particularly to tilt angle optimization, where the propeller tip should be kept on its location and the thruster/pod unit should be rotated about this point. The pod full-scale geometry can be modelled around standard model thruster units. The forces and moments recorded by the transducers in the measuring frame during the tests are to be processed in a standard manner. Cross-talk corrections and calibrations are linear (to a high degree) for the measurement set-up employed.

Prior to each propulsion test, an "in-situ" static load test should be carried out. Not only to check the calibration factors for the podded propulsor in the built-in condition, but also to serve as a check that there are no unintended contacts between the pod unit and the ship model, that will affect the propulsion measurements.

6. GUIDELINES ON EXTRAPOLATION TO FULL-SCALE

6.1 Introduction

This section presents an outline extrapolation method for test on ship models equipped with podded propulsor models. It must be noted that special propulsor configurations such as pulling units behind conventional propellers in a hybrid contra-rotating combination, and podded propulsors with nozzles (rim or hub driven) are left out as future work due to their limited applications.

Power prediction procedure of a vessel with podded propulsion systems is basically the same as for a vessel with conventional propulsion systems. However, there are further complexities associated with scale effect of a podded propulsor that can be investigated under the scale effect (Reynolds number) of the propeller blades and scale effects of the pod housing drag. The treatment of the scale effect of the propeller blades is the same as a conventional propeller and can be corrected by the method proposed in the ITTC'78 Extrapolation Procedure. The scale effect of the pod housing drag is more complex and several empirical correction methods have been presented by different establishments; discussed in details by the 24th ITTC Pod Committee **ITTC (2005)**. A summary of these empirical methods is presented in Table 6.1. In addition to the above empirical methods, Krylov Ship Research Institute (KSRI) presented another simple method using scaling factor α (full scale/model scale) based on CFD calculations by **Lobatchev and Chicherin (2001)**.

Establishment	HSVA	MARIN	SSPA	SUMITOMO
Number of calculation zones	3 (4)	3	3	3
Frictional Resistance calculation method	Schoenher	ITTC 1957	ITTC 1957	ITTC 1957
Pressure Resistance calculation	No	form factors	form factors	form factors
Strut- pod body interaction	No	No	Yes	Yes
Inflow velocity components	Axial only	Axial only	Axial only	Axial only

Table 6.1: A summary of existing semi-empirical correction methods for pod housing.

Based upon the investigation conducted by the 24th and 25th ITTC Specialist Committees it is recommended that the power-speed prediction of a pod driven vessel in full-scale can be conducted using a similar procedure as in procedure 7.5-02-03-01.4 '*1978 propulsion prediction method for single screw ships',* with special care involving the podded-propulsor

hull interaction and pod housing drag correction as described in the following sections.

6.2 Extrapolation method of wake fraction

For wake extrapolation, it is recommended to regard the complete pod unit as the propulsor. The advantage of adopting this approach is that the scale effect on the hull wake can be treated similar to the wake for conventional propellers.

It is generally recognised however that the scale effect on hull wake for a ship propelled using puller type podded propulsors is small, typically twin screw ships with open aft end arrangements.

Exceptions however do exist, such as a tanker or a bulk carriers fitted with a stern bulb where the scale effects on the wake are significant and normal wake scaling procedures are therefore applied. Therefore the existing extrapolation methods of wake fraction such as procedure 7.5-02-03-01.4 '*1978 propulsion prediction method for single screw ships',* can be applied without any modification.

6.3 Extrapolation method of pod housing drag

As stated earlier, there are several methods for pod housing drag correction and differences in these methods have been reported to be considerable, **ITTC (2005)**. However further investigation by the 25th ITTC Pod Committee revealed that the effect of the differences of optimistic power prediction method and pessimistic one on the final power is expected to be less than 2%. Based on this, it is justifiable to apply a simple method to predict the pod housing drag in full-scale and associated correction procedure as a part of a practical power prediction exercise.

In the following a semi-empirical method for such purpose is described. The pod housing drag including the effect of propeller action can be assumed to be:

$$\Delta R_{POD} = \Delta R_{BODY} + \Delta R_{STRUT} + \Delta R_{INT} + \Delta R_{LIFT}$$

Where, B_{BODY}, R_{STRUT}, R_{INT} and R_{LIFT} are components of the resistance associated with pod body (nacelle), strut, pod body-strut interference and lift effect due to swirling flow action of the propeller, respectively.

For well-streamlined pods and lightly loaded propellers, R_{LIFT} may be neglected without affecting significantly the unit thrust. Heavily loaded propellers (low advance ratio) combined with thick pod diameters may need special treatment for $R_{LIFT.}$

By using the form factor approach, which has been proposed in open literature as shown in Table 6.1, R_{BODY} and R_{STRUT} can be represented in the following manner;

$$R_{BODY} = (1+k_{BODY})\, R_{BODY}$$

$$R_{STRUT} = (1+k_{STRUT})\, R_{STRUT}$$

Where (1+k) is appropriate form factor described in Section 6.2.1 and 6.2.2, R_F is frictional resistance of the respective component

Interference drag, R_{INT} can be represented by the following semi-empirical formula **Hoerner (1967)**.

$$R_{INT} = \frac{1}{2}\rho V^2 t^2 f\left(\frac{t_{root}}{C_{root}}\right),$$

with

$$f\left(\frac{t_{root}}{C_{root}}\right) = C_{ROUND}\left(17\left(\frac{t_{root}}{C_{root}}\right)^2 - 0.05\right)$$

Where, t_{root} is maximum thickness at strut root and C_{root} is chord length at the same section. C_{ROUND} is correction factor for various fairing and it varies from 0.6 to 1.0.

Although the contribution of the interference drag, $R_{INT,}$ in the total pod drag estimation is important its expression in the above formula is independent of friction and hence there will no scale effect associated with it.

6.3.1 Pod body form factor

There are several empirical methods for resistance prediction of three dimensional stream lined bodies such as airships and hence the associated form factor. It would be reasonable to use such methods and associated formula for predicting pod resistance because the shape of a pod nacelle resembles that of an

airship. One empirical formula frequently used is presented by **Hoerner (1967)**.

$$R_{BODY} = (1+k_{BODY})\left(\frac{1}{2}C_F\rho V^2 S\right)$$

$$k_{BODY} = 1.5\left(\frac{D}{L}\right)^{\frac{3}{2}} + 7\left(\frac{D}{L}\right)^3$$

Where,
S = Wetted surface Area (m^2)
L = Pod length (m)
D = Pod diameter (m)

6.3.2 Strut form factor

The resistance of strut can be presented in the same manner and associated form factor ($1+k_{STRUT}$) is also presented by simple formula by **Hoerner (1967)**.

$$R_{STRUT} = (1+k_{STRUT})\left(\frac{1}{2}C_F\rho V^2 S\right)$$

$$k_{STRUT} = 2\delta_s + 60(\delta_s)^4$$

Where, δ_S is the average thickness ratio of the strut and S is wetted surface area of the strut.

6.3.3 Effect of propeller slip stream

There are two expressions to predict the axial inflow velocity which is accelerated by a propeller given by **Mewis (2001)** and **Holtrop (2001),** respectively, as below:

$$V_{INFLOW} = V_A(1+C_T)^{0.5}$$
$$V_{INFLOW} = a(nP) + (1-a)V_A$$

Where, V_A and n are the advance speed of propeller and propeller shaft speed respectively, P is the average pitch of the propeller blades and C_T is thrust coefficient defined by:

$$C_T = \frac{T}{0.5\rho V_A^2 A_P}$$

Where,
T = Propeller thrust
A_P = Propeller disc area

The first equation can be applied without any empirical factor however, it can be applied only pulling pod. The second equation requires an appropriate value for the empirical factor (a) that can be applied to not only pulling pod (a = 0.8) but also pushing pod (a = 0.25).

6.4 Consideration from pod resistance tests

In order to validate the simple approach for the pod resistance prediction proposed in Section 3.2 and to further discuss some effects of different flow regimes following analysis is presented.

The results of a puller type model pod resistance tests (without propeller blades / action but with dummy hub), which were conducted in seven different model basins via a co-operative testing programme, are compared with the predicted ones based on Section 3.2, as shown in Figure 6. 1, **Veikonheimo (2006).**

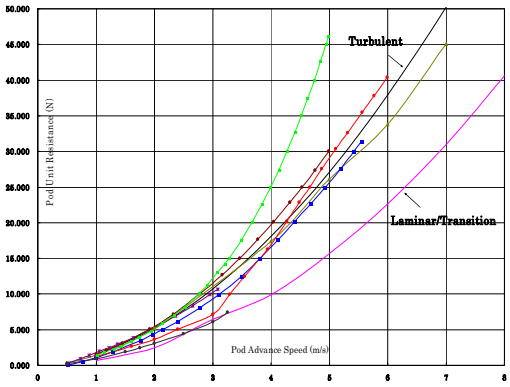

Figure 6.1: Comparison of the pod housing drag from predictions and test results from seven different model basin. **Veikonheimo (2006)**

The main dimensions of the subject pod housing used in this test campaign are given in Table 6.2. Each model basin involved did manufacture their own pod housing/dummy according to the same set of drawings provided although there were slight differences in details of the housing and its towing arrangement.

As shown in Figure 6.1 the predicted drag curves, which are calculated by using two different frictional drag coefficients corresponding to the turbulent and laminar/transition Re number regimes, display expected difference in magnitude. However, significant scatter amongst the test results can be observed with the following distinctive peculiarities:

$$C_F = \frac{1}{(3.46\log_{10}\mathrm{Re} - 5.6)^2} - \frac{1700}{\mathrm{Re}}$$

Table 6.2: Principal dimensions of pod housing used in co-operative testing programme, **Veikonheimo (2006)**

Principal dimensions of Pod Propulsor	
Length of Pod Body	0.4563 m
Diameter of Pod Body	0.1135 m
Height of Strut	0.1372 m
Chord Length of Strut	0.2672 m
Total Wetted Surface Area of Pod	0.2129 m^2

- Below the pod model advance speed of 3 m/s, the maximum and minimum of the measured drag curve lie more or less within the boundaries of the calculated drag curves based on the turbulent and laminar/transition Re number regime, respectively,
- Above the pod model advance speed of 4 m/s, all the results (with the exception of one facility) follow the trend of the turbulent regime drag calculations.

In the prediction of the above mentioned frictional resistance coefficients following empirical formulae are used by taking into account appropriate Re number range.

Laminar or transitional flow regime;

$\underline{Re < 5.25\text{x}10^4}$

$$C_F = \frac{1.327}{R_e^{0.5}}$$

$\underline{5.25\text{x}10^4 \le Re < 2.0\text{x}10^6}$

$$C_F = C_F * 10^{0.117 f(\mathrm{Re})}$$

$\underline{2.0\text{x}10^6 \le Re}$

where,

$$C_F = \frac{1}{\left[3.46\log_{10}(2.0\times10^6) - 5.6\right]^2} - \frac{1700}{2.0\times10^6}$$

$$f(\mathrm{Re}) = \left[\log_{10}\mathrm{Re} - \log_{10}\left(2.0\times10^6\right)\right]^2$$

Turbulent flow regime;

$\underline{Re > 2.0\text{x}10^6}$;

$$C_f = \frac{0.075}{(\log_{10} R_e - 2)^2}$$

In using the above formulae recommendation is to use the laminar/transition regime formulae for the outer zone which is outside the propeller slipstream and turbulent regime formulae for the inner zone.

A comparison of the calculated frictional resistance curves for the subject pod housing for different flow regime and Re number range is shown in Figure 6.2.

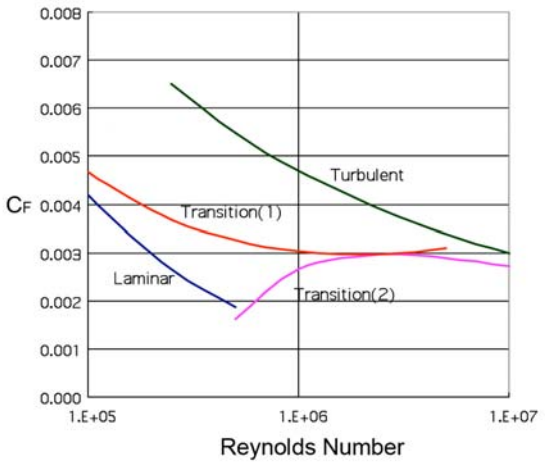

Figure 6.2: Comparison of calculated frictional resistance coefficients (C_F) for the pod housing using appropriate empirical formula for laminar, transitional and turbulent flow regimes

On the other hand the drag coefficient (C_D) for the subject pod housing resistance (R_{POD}) measured by the seven Model Basins and based on the total wetted surface area (S) are given below and comparative curves are shown in Figure 6. 3.

$$C_D = \frac{R_{POD}}{\left(\frac{1}{2}\rho V^2 S\right)}$$

Comparing Figure 6.3 with Figure 6.2 following facts are self-explanatory:

- Below Reynolds number 1.0×10^6, the earlier mentioned large scatter originated from unstable flow fields due to transition regime appears to play a role.

Above Reynolds number 1.5×10^6, all the measured curves except one tend to converge to turbulent flow curve.

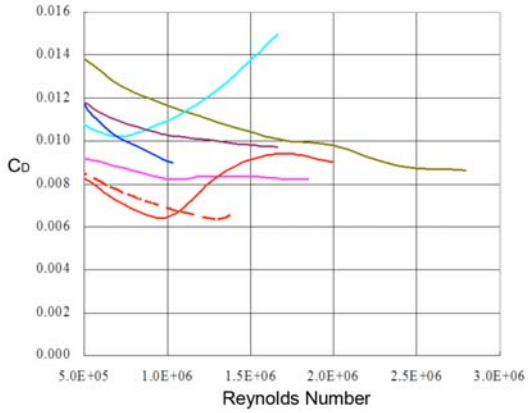

Figure 6.3: Comparison of pod resistance coefficients (C_D) for the pod housing measured by seven model basins, **Veikonheimo (2006).**

6.4 Full scale podded propulsor characteristics calculated by present method

As stated earlier, powering prediction of a vessel fitted with podded propulsor(s) can be treated basically the same as a ship with conventional propeller(s). In essence, the main difference exists only in the definition of propeller efficiency (η_o) term as appears in the propulsive efficiency (η_D) as described below:

$$\eta_D = \frac{(1-t)}{(1-w)}\eta_R\eta_0$$

$$\eta_O = \frac{(J)}{(2\pi)}\frac{K_{TU}}{K_Q}$$

Where non-dimensional thrust coefficient K_{TU} is associated with the pod unit thrust (T_{UNIT}) instead of propeller thrust (T_{PROP})

Non-dimensional unit thrust coefficient (K_{TU}) and torque coefficient (K_Q) at full-scale can be obtained based on the model unit thrust coefficient [$(K_{TU})_M$] and torque coefficient [$(K_Q)_M$] by applying appropriate scale effect corrections in the following manner;

$$K_{TU} = (K_{TU})_M + \Delta K_{TP} + \Delta K_{TU}$$
$$K_Q = (K_Q)_M + \Delta K_Q$$

Where ΔK_{TU} and ΔK_Q are the scale effect corrections associated with drag on the propeller blade thrust and torque, respectively and can be estimated based on ITTC 78 Performance prediction method. ΔK_{TU} corresponds to pod housing drag correction and defined as:

$$\Delta K_{TU} = \frac{\Delta R_{POD}}{\rho n^2 D^4}$$

With

$$\Delta R_{POD} = \Delta R_{BODY} + \Delta R_{STRUT}$$

Where ΔR_{BODY} and ΔR_{STRUT}, as discussed earlier in Section 6.3, can be represented using appropriate frictional drag coefficients and form factors for both model ($_M$) and full-scale ($_S$) values as below.

$$\Delta R_{BODY} = \frac{1}{2}\rho\, S_{BODY}\, V_{PS}^2\, (1+k_{BODY})\{C_{FM} - C_{FS}\}$$

$$\Delta R_{STRUT} = \frac{1}{2}\rho\, S_{STRUT}\, V_{PS}^2\, (1+k_{STRUT})\{C_{FM} - C_{FS}\}$$

As stated in Section 3 there are several pod housing drag correction methods, these are summarised in Table 6.3. In order to compare the extrapolation method presented in this section with some of the methods included previously in Table 6.3, the propulsor from the co-operative research programme was adopted as the propulsor for the case study. The pod housing drag values for this propulsor were then estimated in the model and full-scale and are given in Table 6.3.

The experimentally measured values for the total pod housing drag are also included in this comparative analysis including the minimum and maximum recorded values (EXP_{min}, EXP_{max}) also shown in Table 6.3.

Table 6.3: Comparative analysis of pod housing drag predicted by the present and other methods

V= 3.25 m/s MODEL SCALE

	Rpod(N)	R_body(N)	R_strut(N)	R_btmfin(N	Rint_strut(N	Rint_bfin(N)
ITTC	9.13	3.38	2.99	0.58	2.03	0.16
A	8.18	3.34	2.99	0.60	1.14	0.11
B	5.27	2.66	2.26	0.35		
C	6.45	2.37	1.64	0.27	2.03	0.16
EXPmin.	8.17					
EXPmax	13.38					

	Rpod	R_body	R_strut	R_btmfin	Rint_strut	Rint_bfin
ITTC	6.4%	2.4%	2.1%	0.4%	1.4%	0.1%
A	5.7%	2.3%	2.1%	0.4%	0.8%	0.1%
B	3.7%	1.9%	1.6%	0.2%	0.0%	0.0%
C	4.5%	1.7%	1.1%	0.2%	1.4%	0.1%

V= 11.83 m/s FULL SCALE

	Rpod(KN)	R_body(KN	R_strut(KN	btmfin(KN	Rint_strut(KN	Rint_bfin(KN
ITTC	44.63	13.16	11.24	1.99	16.94	1.30
A	46.76	13.01	11.25	2.06	18.60	1.84
B	20.04	10.17	8.34	1.52	0.00	0.00
C	34.97	14.14	11.24	1.99	7.06	0.54

	Rpod	R_body	R_strut	R_btmfin	Rint_strut	Rint_bfin
ITTC	3.8%	1.1%	1.0%	0.2%	1.5%	0.1%
A	4.0%	1.1%	1.0%	0.2%	1.6%	0.2%
B	1.7%	0.9%	0.7%	0.1%	0.0%	0.0%
C	3.0%	1.2%	1.0%	0.2%	0.6%	0.0%

In Table 6.3 the present method is denoted by ITTC whilst the other three existing methods are denoted by A, B and C. In this table, the total pod housing drag is also given in terms of its sub-components due to the pod body (nacelle), strut, bottom fin, body-strut interaction and body-bottom fin interaction terms. The predicted full-scale data corresponds to a ship speed of 11.83 m/s corresponding to a model scale speed of 3.25 m/s based on a scale factor of λ=13.25. In Table 6.3, both the model and full-scale values are presented in terms of the actual resistance values in the top sub-table and a percentage ratio of each respective drag component to the total unit thrust (e.g. 100 x R_{POD} / T_{UNIT} as displayed in the first column) in the bottom sub-table.

In Table 6.4, the unit thrust (T_{UNIT}) and pod housing drag (R_{POD}) are estimated in full-scale using the model test data and present pod housing drag correction method and results are displayed in comparison with the available full-scale data. The top sub-table of Table 6.4 displays the actual thrust and pod drag values whilst the second column of the bottom sub-table displays the percent ratio of the pod drag to unit thrust (i.e. 100 x R_{POD} / T_{UNIT}).

Table 6.4: Effect of propeller action on housing drag

	T_{UNIT}	R_{POD} / T_{UNIT}
Model Scale (present)	139.6kN	11.4%
Full scale (direct)	1165.0kN	94.8%
Full scale (present)	1165.0kN	75.8%
Ratio		0.799%
Model Scale (present)	139.6kN	8.1%
Full scale (direct)	1165.0kN	8.1%
Full scale (present)	1165.0kN	6.5%

In reviewing the findings from Table 6.3 and Table 6.4 it can be seen that in Table 6.3, the comparison of the percent pod housing drag to unit thrust values between the model and full-scale using different drag correction methods display differences at about 1-3% depending upon the correction method selected. However in Table 6.4, the comparison of the percent pod housing drag to unit thrust predicted with the direct measurement in full-scale displays 2% difference.

6.5 Effect of propeller slipstream

The pod housing drag increases behind a propeller due to action of its slipstream. Consequently, the pod unit thrust will decrease as the pod drag increases. As shown previously in Table 6.4, a comparison of the pod-housing drag coefficient for the model to full-scale defined by:

$$\alpha = \frac{K_{calc\,(\text{full scale housing})}}{K_{calc\,(\text{model scale housing})}}$$

Where,

K_{calc} = non dimensional pod housing drag coefficient calculated using the present method. This can be considered to be the ratio of the

pod housing drag to the unit thrust in the above table.

Therefore using the above:

$\alpha = 6.5/8.1 = 0.799$ for the case study pod.

6.6 Considerations from CFD Methods

6.6.1 Short review of CFD methods

Since the last ITTC general meeting the literature on CFD applied to podded propulsors has continuously been increasing. Some of this work was reported in the 2nd T-Pod conference held at L'Aber Wrac'h, France in 2006. Potential-flow methods have been used either alone **(Greco et al. 2006, Ma et al. 2006, Bal et al. 2006)** or in combination with RANS/Euler equation methods **(Ohashi and Hino 2004, Mishra 2005, Kinnas et al. 2006, Krasilnikov et al. 2006, Deniset et al. 2006, Lovatchev 2008, etc)** to simulate the hydrodynamics effects on the propulsor. Pure RANS simulation has been employed also **(Sánchez-Caja et al., 2003 & 2006)**.

Within inviscid flow theory the flow around the pod housing has been modeled by panel methods **(Nakatake et al. 2004, Islam et al. 2004, Deniset et al. 2006)** or Euler solvers **(Gupta 2004, Mishra 2005, and Kinnas et al. 2004 & 2006)**. Among the effects investigated are the interaction between propeller and pod housing, flow unsteadiness, wake alignment, forces on various parts of the housing and propeller, etc. However, inviscid theory is unable to treat properly the scaling of forces, which is a direct consequence of viscous effects.

For the study of scale effects on drag RANS methods have been used instead in the form of either hybrid viscous-potential methods or pure RANS methods. Hybrid viscous-potential methods use potential theory for modeling the propeller in terms of actuator disk / lifting line models **(Lovatchev et al., 2001 & 2008)**, lifting-surface vortex-lattice models or panel methods **(Krasilnikov et al. 2006)**. On the other hand the flow around the pod housing is simulated by solving the RANS equations. **Ohashi and Hino (2004)** presented a hybrid RANS method with an unstructured grid for hull flows where CRP propellers were modeled by body forces. Scale effects on pod resistance have been investigated by an hybrid approach in **Lovatchev et al. (2001 & 2008)** and by pure RANS solvers for the complete propulsor unit in **Sánchez-Caja et al., (2003 & 2006)**.

6.6.2 RANS methods applied to scaling

During the last decade detailed analysis of the complex flow around podded propulsors has been carried out and partly reported for computations made at model and full scale. Phenomena such as flow separation on pods and struts, propeller-housing interaction etc., have been numerically studied. However, many open questions about the behaviour of various turbulent models are still unsolved in part due to the lack of validation data at full scale. In particular, variations in viscous pressure drag due to changes in scale need further study and validation.

Full-scale validation data are not available for many of the outputs resulting from RANS computations due mainly to the complexity involved in the measurements. This is a problem when judging the reliability of RANS predictions. However, a careful and critical analysis of the RANS results may help to identify some flow phenomena of interest for the extrapolation.

In particular regarding R_{LIFT}, it is generally accepted that R_{LIFT} can be calculated within the framework of potential-flow theory and that the non-dimensional lifting forces at model-scale are valid at full scale. However, it should be mentioned that for struts with rounded and thick trailing edges (TE), flow separation at model scale plays an important role in the reduction of lift. CFD calculations suggest that for some applications the strut lift may be increased at full scale due to the reduction of TE separation (about 1 % of the unit thrust for the case in Figure 6.4).

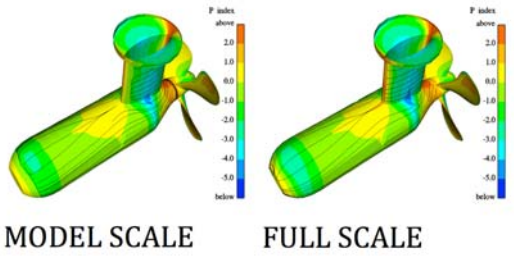

Figure 6.4: Pressure distributions and streamlines on pod housing/strut surfaces at model and full scale **Sanchez-Caja, et al. (2003)**

In the same reference the scaling of drag for a pod body with a blunt aft-end is numerically investigated. The scaling of the frictional forces seems to follow the expected trend of frictional drag reduction at full scale. However, the scaling of the pressure forces seems to contradict the trend expected in an extrapolation method based on form factors.

Within the form factor approach, the scaling of pressure drag is assumed to follow the ratio of the frictional coefficients for all types of bodies, i.e:

$$\frac{C_{\mathrm{T\,(Full\,Scale)}}}{C_{\mathrm{T\,(Model\,Scale)}}} = \frac{(1+k)\;C_{\mathrm{f\,(Full\,Scale)}}}{(1+k)\;C_{\mathrm{f\,(Model\,Scale)}}} = \frac{C_{\mathrm{f\,(Full\,Scale)}}}{C_{\mathrm{f\,(Model\,Scale)}}}$$

In principle, the form factor approach has been devised for well-streamlined bodies where ideally no separation occurs, and is supposed not to work very well for bodies with extensive separation. Blunt aft-end pods are somewhat similar to projectiles. Projectiles develop a large pressure drag at their aft-end, called '*base*' drag, which follows different scaling laws due to the generation of strong vortices on the sharp shoulders. In the past some institutions have treated this drag component in hull resistance extrapolation of small crafts abandoning the form factor scaling law. They have assumed that the pressure drag coefficient is the same at model and full scale (in other words, is not reduced at full scale following the ratio of the frictional coefficients).

In the referenced CFD calculation **Sanchez-Caja, et al. (2003)**, the pressure drag for the blunt aft-end pod body is seen not to decrease in full scale following the reduction of frictional coefficients from model to full scale, but to increase somewhat. The increase in pressure resistance predicted by CFD is in line with the trend found in experiments of increase in base drag with the Reynolds number. This result points also to the direction that it is not adequate to reduce pressure drag at full scale by the ratio of frictional coefficients for pods with blunt ends, and that it should be given to such pod shapes a special scaling treatment.

CFD calculation exercise

A calculation exercise has been made in order to apply extrapolation factors obtained by CFD to the pod case shown in Tables 4 and 6.5. The extrapolation procedure is explained in **Chicherin et al. (2004)**. The computations were performed at KSRI and VTT following a different computational approach. A scaling factor is established as ratio of computed full scale and model housing thrust coefficients:

$$\alpha = \frac{K_{calc\,(\text{full scale housing})}}{K_{calc\,(\text{model scale housing})}}$$

Table 6.5: Main data for the CFD study case

	Model scale	**Full scale**
Propeller diameter	0.231	5.8
Propeller revolutions (rps)	16	2.33
Advance coefficient	0.88	0.88
Reynolds number (model)	$1.29x{\cdot}10^{6}$	$1.14{\cdot}10^{8}$

KSRI used a RANS code combined with an actuator disk model for the simulation of the propeller. To close the RANS equations, KSRI code used a high-Reynolds k-epsilon turbulence model. The flow upon the entire pod housing is considered turbulent. A purpose-developed system of wall functions enabled to use a comparatively sparse mesh near the wall within a wide range of Reynolds

numbers. In this exercise, the mesh consisted of 0.6 million cells. The effect of the propeller upon the pod was simulated in the RANS procedure by body forces, i.e. the solver used the actuator disk model with flow swirling. The intensity of the body forces simulating the propeller was specified based on a given propeller thrust and torque values found from open-water tests of thruster unit. This method is described in **Lobatchev, et al. (2001)** and **Chicherin et al. (2004)**. The loading is not calculated but fixed to the value obtained from model tests.

VTT used RANS code FINFLO with a full modeling of the actual geometry of the propeller and pod housing. Chien's k-epsilon turbulence model was used in the calculation. The solution was extended to the wall, i.e. no wall functions were employed. The mesh consisted of about 6 million cells. The propeller loading was calculated as an output of the computation. The numerical approach is described in **Sanchez-Caja, et al. (2003)**.

A summary of the conclusions resulting from this exercise is as follows. VTT and Krylov RANS codes followed different computational approaches to the problem, and they gave also different absolute results for the pod housing drag coefficient. However, the relative differences model versus full scale drag were represented by scaling factors of 0.655 for KSRI and 0.75 for VTT. These scaling coefficients yield a prediction of K_{Tunit} of about 1% difference within the extrapolation of model scale test results to full scale.

For the purpose of comparing CFD approach to the method suggested by our Committee an equivalent scaling factor was calculated for the same pod case using the recommended procedure as described in Sections 3.1-3.4. A factor of 0.79 was obtained. Table 6.5 compares the results obtained by direct CFD simulation at full scale with those obtained following the ITTC recommended method. The CFD-based scaling factor method should give results similar to the recommended simplified procedure for pods with streamlined body.

A direct comparison of CFD results was also made with model experiments and some limited full scale measurements. For the comparison the calculations made with full modelling of propeller and housing (VTT) were taken. Figure 6.5 shows in percentages the range of dispersion in thrust and torque coefficients and in efficiency for model scale experiments together with the CFD predictions. The value 100% corresponds to the mean between the maximum and minimum value obtained in the tests from the facilities participating in the experimental campaign. The computed torque and thrust were below the range in the model scale experiments. The model scale efficiency was within the range. It should be noticed that the calculations assumed fully turbulent flow at model scale, which means larger frictional coefficients in the absence of separation.

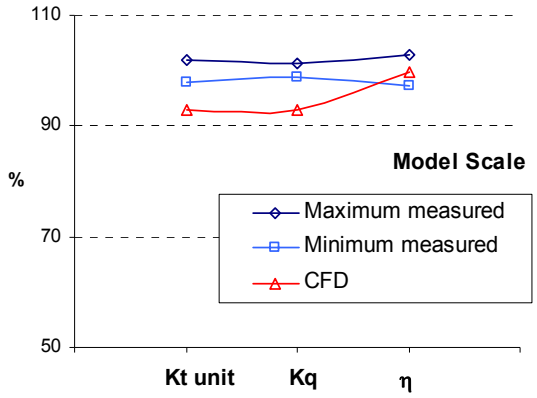

Figure 6.5: Range of performance coefficients from model scale experiments versus CFD predictions.

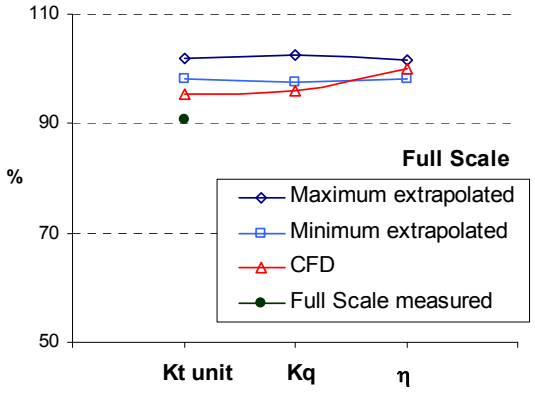

Figure 6.6: Range of performance coefficients extrapolated to full scale by different model basins versus CFD predictions.

Figure 6.6 shows in percentages the performance coefficients extrapolated to full scale from the experimental facilities compared to the results from the CFD computations. Full scale K_{Tunit} is also given. At full scale the computed efficiency fell within the dispersion range of the predictions made by the institutions participating in the experimental campaign. The thrust and torque were somewhat smaller. The difference in computed K_{Tunit} at full scale from ship measurements was 5 percent. On the other hand the mean value of the extrapolations made by the experimental facilities was about 9-10 percent above the experimental one. In this particular case the full scale CFD calculation yields better result than estimations based on model scale experiments. Finally Table 6.6 compares the results obtained by direct CFD simulation at full scale with those obtained following the ITTC recommended method. The drag of the different components of the pod unit is expressed as percentages of the blade thrust.

Table 6.6: Comparison of results from direct CFD and ITTC simplified method on pod housing drag calculations

	Direct CFD	ITTC simplified procedure
Blades	100.0 %	100.0%
Strut+ uppermost body	-4.6%	-2.7%
Pod body	-2.9%	-2.9%
Fin	-0.2%	-0.5%
TOTAL(unit thru	92.4%	93.9%

7 QUESTIONNAIRES

7.1 Summary of the Responses

The questionnaires were sent out to forty major ITTC member organizations. Twenty organizations from twelve countries responded with almost full answers. Compiling the all replies from major organizations worldwide, this report briefly summarizes the survey results. Responses are analyzed in the following sections, with number of organizations indicated in parenthesis.

7.2 Analysis of the Responses

Propeller Open Water Test

As a first step, the questionnaire for this part is given to compare the results on normal propellers with these on the open water test of podded propulsors. Major questions are related to the specifications of the POWT measurement system and propeller models. All of organizations use their towing tanks for POWT and the diameter of the tested propeller models mainly ranges from 150mm to 300mm. Eleven organizations conduct the POWT at several revolution rates of tested propeller models to check the Reynolds number effects carefully.

Three organizations use the propeller models larger than 300mm in diameter. Most of them (18) usually use the model of the diameter between 200 and 300mm as their own standard size. Four organizations use the propeller diameter less than 150mm and the tested minimum diameter of propeller model is 70mm.

Most of organizations (14) make the Reynolds number effect correction on the measurements by using the ITTC 1978 methodology. Five organizations have no standard Reynolds number, while other fourteen organizations perform the POWT at the standard Reynolds number based on the propeller diameter from 5×10^5 to 10^6.

Nine organizations consider no serious problems on the prevention of air-drawing at the POWT but other ten take individual measures to prevent the propeller from air-drawing. Thirteen organizations perform the POWT at the propeller immersion more than 100% Dp and half of respondents (12) do it at more than 150% propeller immersion.

Podded Propeller Open Water Test

Replies to this part are not unique, compared with those of the previous part.

Currently, the Podded POWT is conducted with the own methods of very distinctive individualities. Especially, the answers to the questionnaire about the method to fix the POD dynamometer have wide variety. This reflects the fact that there are no well-established test procedures in the field of podded propeller open water test.

Nine organizations employ a shallow draft boat, while five and four organizations attach an end plate and flat plate to the podded propeller dynamometer to carry out the podded POWT, respectively as shown in Figure 7.1. All of response organizations (17) measure the forces against the entire pod load cells as well as the thrust and torque of propeller, to understand the interaction between propeller and pod casing.

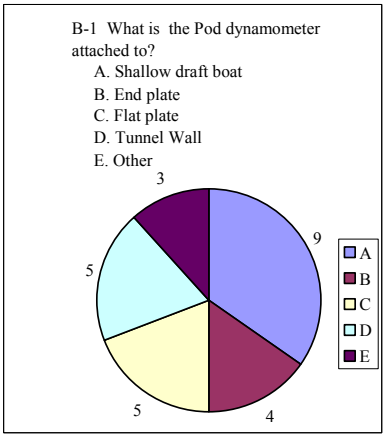

Figure 7.1: Fixing Method of Pod Dynamometer

The width of gap between propeller hub and pod housing is also arbitrarily chosen by each organization as shown in Figure 7.2. As the width of the gap has some influence on the measured propeller thrust, basic consensus on the gap width in the test might be required. The Reynolds effect on the propeller performance of podded propulsors is more

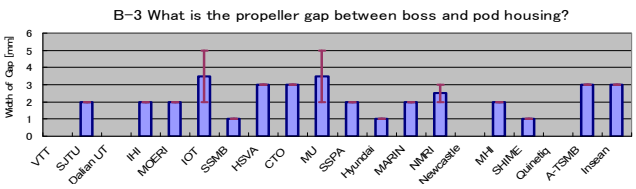

Figure 7.2: Survey Results of Gap Width

decisive than the gap effects. Fourteen organizations perform the measurement at the gap between two and five mm and twelve organizations adopt the absolute own gap, two or three mm, regardless of the size of propeller models empirically. One organization performs the measurements with the width determined by the tested propeller model diameter. The criteria for reasonable gap width should be established based on scientific efforts. Most of podded propeller dynamometers (15) are driven by the motor equipped to the outside of the dynamometer and sixteen organizations install the thrust and torque sensors in the pod casing to measure the propeller performance.

Seven organizations perform the podded POWT at only one standard propeller

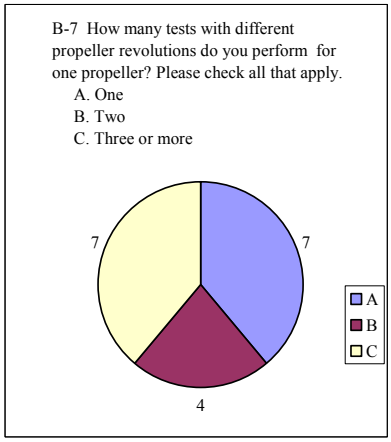

Figure 7.3: Survey Results of Propeller Revolution Number Effects

revolution rate or that for the self-propulsion test, while eleven organizations conduct the measurements at two or three revolution rates including the rate determined by the maximum capacity of the dynamometer as shown in Figure 7.3. The same results are obtained as the POWT.

The podded POWT is performed by nine organizations mainly at the propeller immersion which ranges from 150% to 200% D_P of the tested propeller model (Figure 7.4). The propeller immersion for the Podded POWT is deeper than that of the normal POWT in some organizations as described in the previous section. Six organizations conduct the Podded POWT at the smaller propeller immersion which ranges from 100% to 150% D_P.

Resistance & Self Propulsion Test

The most interesting topics on this part are an experimental procedure and a data analysis method. Resistance and self-propulsion tests are conducted by two major analysis methods, that is, the propeller base method and the unit base method. Each method has some merits and demerits. From the analysis of the questionnaire, almost half of organizations (11) employ only the unit base analysis for the resistance and self-propulsion tests and six organizations also perform the tests by using both the propeller base and the unit base analysis methods. Only two organizations conduct the resistance and propulsion tests by a conventional propeller base method which treat the pod casing as the appendage of a hull as shown in Figure7.5.

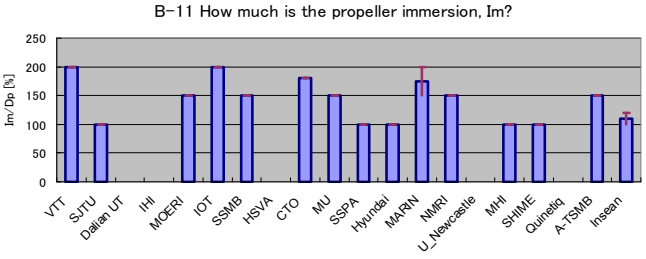

Figure 7.4: Survey Results on Propeller Immersion

The roughness correction for a podded propulsion ship hull without the pod propulsor is made by using the same value as that for a conventional ship hull form by seven organizations.

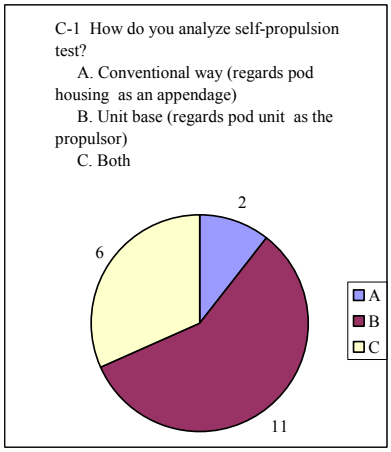

Figure 7.5: Survey Results on Propulsion Analysis Methods for Pod Propulsion Ships

The calibration of the podded propulsor dynamometers is made in a statically loaded manner by most of the organizations (18) and three organizations carry out the calibration dynamically.

Powering

A reliable scaling method for predicting the full scale propulsive performance of pod propulsion ships have not established yet. The important issues are to predict the drag of the pod housing and the effective thrust of podded propulsors in full scale.

Most of the organizations (14) asses the Reynolds effects on the performance of a podded propulsor for the powering of pod propulsion ships. The correction methods for the pod housing drag are based on CFD, an empirical method, semi-empirical methods, Only two organizations use CFD for the pod housing drag corrections, while seven organizations employ individual semi-empirical methods and the corrections by other four organizations are based on empirical or experimental methods as shown in Figure 7.6 (a).

Nine organizations make the propeller thrust correction for the powering by various kinds of own methods and three of them employ the ITTC-78 method. Only one uses CFD for the propeller thrust correction of the podded propulsors

Fourteen organizations take account the wake scaling effects into the powering of pod propulsion ships as shown in Figure 7.6(b). Seven organizations use the ITTC recommended method, while five employ Yazaki's or Sasajima's methods for the wake scale effect correction.

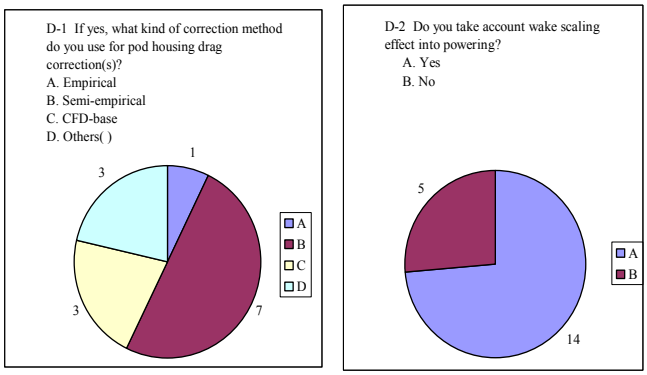

(a) Pod Housing Drag (b) Wake

Figure 7.6: Survey Results on Rn Correction Method

CFD Application

CFD is expected one of the most promising and potential tools for practical application to predict the drag and thrust of the podded propulsor in full scale and to scaling from model to full scale.

Seventeen organizations use to apply CFD for the practical purposes. Seven organizations apply CFD for the scaling and propulsor design. Nine use it for the propulsor and hull interaction as shown in Figure 7.7(a). Almost half of organizations introduce k-εtype or similar turbulence model (RNG, Shin, Lien cubic, Launder-Sharma, Lien-Leschziner etc.) into their computational program codes, while a few use Baldwin-Lomax or its derivatives and/or Spalart-Allmaras or similar one-equation models. Three still employ a potential theory instead of N-S solver as shown in Figure 7.7 (b).

For the computation of the podded propulsor and hull interaction, twelve organizations employ the body force method and four organizations do an infinite bladed propeller theory. As more highly advanced tools, nine and seven organizations utilize a lifting surface theory and a lifting body theory, respectively. Eight organizations use RANS codes as shown in Figure 7.7(c). Fifteen organizations solve the interaction problem between propeller and pod housing by CFD codes. Most of the codes include the tangential flow effects of the propeller induced velocities.

Special Theme

The questionnaires for this part are related to recent concerned issues on the podded propulsors. The hybrid CRP pod propulsion is expected to be one of the most efficient ones but only four perform the open water test for the hybrid CRP propulsion system in a towing tank, using a POWT boat for the forward propeller and a usual podded propulsor dynamometer for the aft propeller. Two organizations replies own correction methods to eliminate or correct the wake from the propeller open boat to the forward propeller. For Podded Tandem Propellers, only one organization has a special instrument to measure the propeller performance. Three organizations carry out the measurement of the thrust and torque of individual propellers separately, while other three do it totally.

To investigate the ice contact problems between a podded propulsor and ice, three organizations have a special instrument to measure the propulsive performance of a podded propulsor working in ice water. Two of them perform the experiment to evaluate the strength of propeller blades and other do to evaluate the cavitation behaviour.

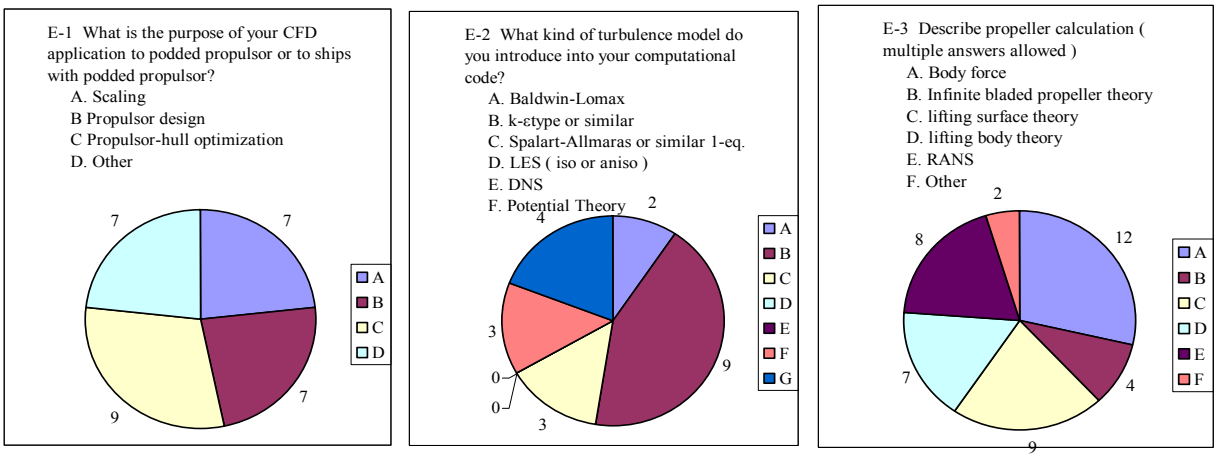

(a) Purpose (b) Turbulence Model (c) Propeller Theory

Figure 7.7: Survey Results on CFD Application

Summary

Questionnaire results indicate that a number of organizations perform the podded propulsor open water test in a towing tank with taking account into Reynolds effects and sufficient propeller immersion. To analyse the propulsive performance of pod propulsion ships, most of organizations use the unit base method. The unit base method is inevitable to predict full scale performance but the propeller thrust and torque information from the podded propulsor dynamometer are more reliable than those from the multi-force balances to design the final propeller. The air-drawing around a podded propulsor should be eliminated completely to obtain reliable data in the propulsion test.

8 REVIEW AND ANALYSIS OF CAVITATION BEHAVIOUR OF PODDED PROPUSORS UNDER THE EFFECT OF POD STEERING ANGLE

8.1 Overview

Task 3 of the committee is *to review and analyse the cavitation behaviour of podded propulsor with emphasis on high pod angles and normal steering angles including dynamic behaviour. Practical application of computational methods to prediction and scaling of the behaviour will be included.*

Since the report of 24th ITTC Azimuthing Podded Propulsion Committee, **ITTC (2005)**, there has been a limited experimental work reported in the open literature while at the same time there is hardly any numerical work reported on the same topic. The following review and analysis therefore report on the recent relevant investigations, after the report of the 24th ITTC, for the effect of steering angles, on the pod propulsor behaviours, focusing on the cavitation but also including the loads and hull pressures.

8.2 Review of the experimental investigations

The complexity of the loading (e.g. manoeuvring loads), cavitation behaviour and fluctuating hull vibrations associated with podded drives has meant that nearly all of the published hydrodynamic research in this field has been pursued using physical model testing. Limited accounts of full scale observations and numerical studies do however exist to help explain the cavitation experienced by a podded propulsor in service.

In addressing this lack of numerical modelling and full scale evidence, **Friesch (2004)** conducted cavitation tests on a typical puller type podded propulsor with static pod angles between ±6°. He found that under steering conditions the cavitation behaviour of the pod changed significantly due to increased blade loading. At some degrees of pod azimuth angles, the drop in pressure at the suction side of the strut caused erosive cavitation to develop inferring that strut geometries with asymmetric profiles would remedy the situation. In general, however, the effect of steering angle on the pressure fluctuations were reported to be remarkable even for small increase and found to be sensitive to the direction of rotation of the propeller, as shown in Figure 8.1.

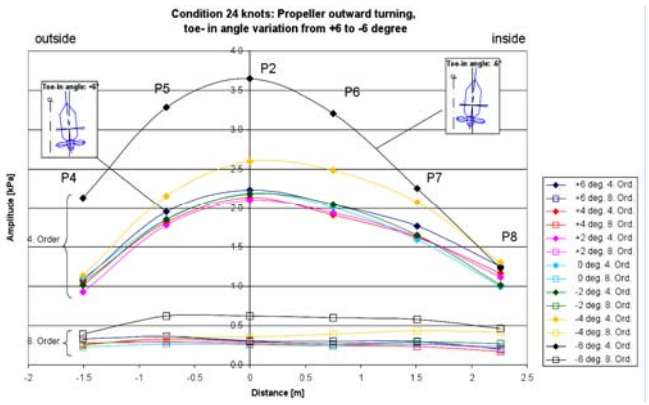

Figure 8.1: Effect of Toe angle on hull pressures, **Friesch (2004)**

In the 24th ITTC report it was suggested that, for normal helm actions (±15°), the cavitation was estimated as low risk since the propeller was yawed together with the pod housing and hence the axial component of the induced velocity in the propeller slipstream was in-line with the strut. For extreme steering angles of 15°-35°, the cavitation risk was high due to the forward speed loss and hence increased

propeller load together with the increased oblique flow incidence.

A useful full scale evidence for the above hypothesis is given by **Pustoshny and Kaprantsev (2001)** for a cruise vessel fitted with twin puller pods for various off-design conditions. Pustoshny and Kaprantsev noted that the cavitation increased in severity with changes in helm angle; at helm angles of 35°, heavy sheet cavitation covered more than 180° of the blade rotation. When the helm action pulled the pods in (from side to centreline) during the dynamic steering action, sheet cavitation covered the whole upper portion of the blade (typical in turning circle manoeuvres). When the helm action was opposite such as when the pods were slewed from centreline to port or starboard (i.e. from centreline to side), the characteristic suction side tip vortex moved from the suction side to the pressure side and then returned back to the suction side as sheet cavitation developed. It was also suggested that careful analysis was required of the wake induced propeller inflow velocities, instantaneous propeller inflow angles under the effect of the drift and propeller revolutions etc.

Other useful cavitation analysis was reported by **Wang et al. (2003)**, who published an experimental study for the effect of static azimuth angle (up to ±30°) on the loading and cavitation behaviour of a puller type podded propulsor of a supply vessel. The cavitation observations at 0° azimuth angle indicated that the model propeller experienced strong tip vortices with growing thickness around TDC. At 15° steering there was a noticeable increase in cavitation intensities compared with other smaller pod angles and the increase and decrease caused by the oblique flow were more noticeable. By 30° azimuth there were significant changes in the cavitation pattern with a large spread of sheet cavitation and intensity caused by the oblique flow effect, as shown at the enlarged window in Figure 8.2. There were also differences in the intensity of the cavitation observed with the port and starboard pod yaw angles.

However one of the most interesting observations at large pod yaw angles was the deformed (rather like elliptical) trajectories of the propeller tip vortices at the extreme pod yaw angles in compared to circular trajectories at zero and smaller yaw angles as shown in Figure 8.2.

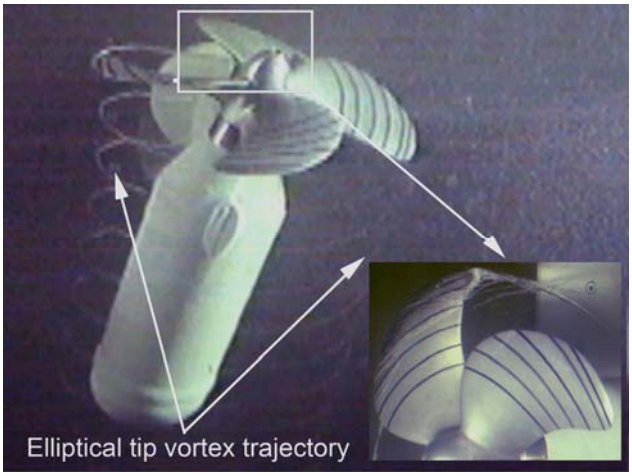

Figure 8.2 : Blade cavitation (on the left) and deformed trajectory of tip vortices (on the right) at 30° pod steering angle, **Wang et al. (2003)**

While most of the published cavitation research into podded drives is for low to medium vessel speed regimes research investigations for the FP5 project, FASTPOD shed interesting and useful light on the cavitation behaviours of high-speed puller type multiple pods with and without the steering flaps. A 40 knot Ropax vessel was driven by four puller type pods; the 2 pods at the front (centre pods) were fixed; 2 pods at the rear (wing pods) were steerable as shown in Figure 8.3.

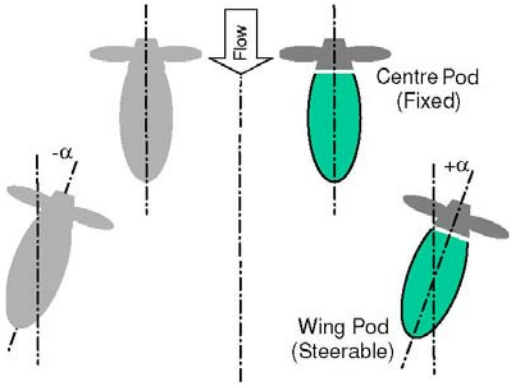

Figure 8.3 : FASTPOD Ropax four pod arrangement, **Johannsen and Koop (2006)**

Comprehensive and rather challenging cavitation tunnel tests were reported by **Johannsen and Koop (2006)**. The tests

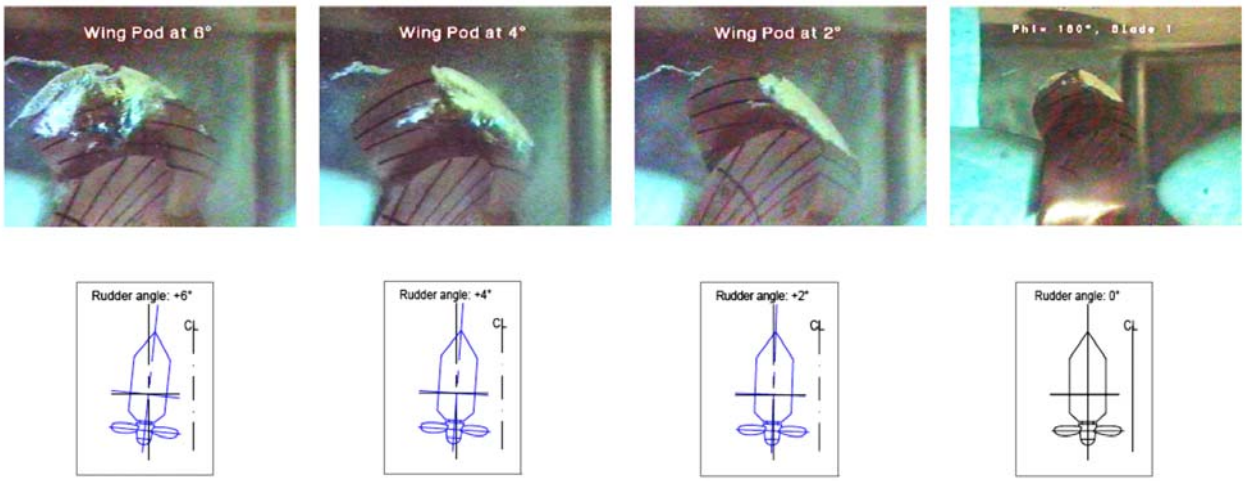

Figure 8.4: Effect of steering angle on blade cavitation, **Bretschneider & Koop (2005)**

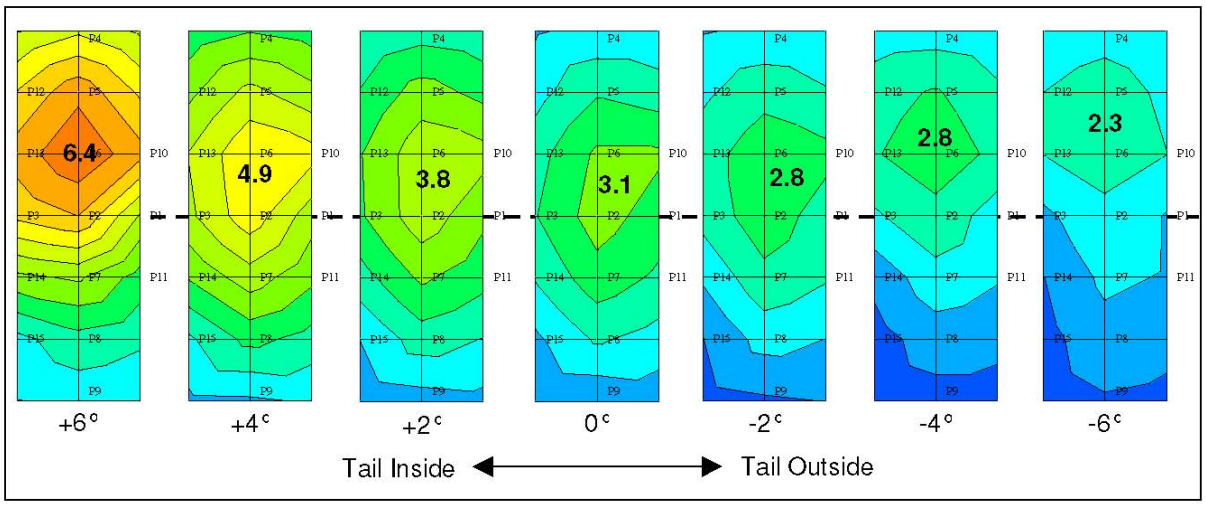

Figure 8.5: Effect of steering angle on hull fluctuating pressures, **Johannsen & Koop (2006)**

observed the cavitation patterns as well as measuring the fluctuating hull pressures and propeller noise at static pod azimuth angles of 0° - 6°. The cavitation behaviour of the fixed centre pod unit (zero yaw) was judged to be acceptable. When the wing pod was at zero yaw angle, the maximum cavitation extent was at TDC where its behaviour was rough, partially cloudy and erosive in nature. When the wing pod was set at normal steering angles applied for course keeping (+/- 3 deg), the cavitation patterns on the blades were rather stable but beyond this range the cloudy and erosive sheet cavitation was dominant as shown in Figure 8.4. No cavitation was observed on the pod housing up to +6° when the pod slewed trailing edge inward. However when the pod slewed trailing edge outward foaming sheet cavitation appeared at the inner side of the pod and by – 6° this foamy cavitation pattern covered more than 50% of the inner side of the strut. At the tail of the pod lower body vortex cavitation was reported that was similar to a heavily loaded propeller hub vortex cavitation. Finally, hull pressure measurements clearly showed the effect of pod steering angles on the hull pressures although the trend in their magnitude and distribution were different depending upon the direction of the steering angle due to the interference caused by the slipstream of the forward pod as shown in Figure 8.5.

Another high-speed vessel, tested in FASTPOD was a 35 knot Container Ship again driven by four puller pods and reported in **Allenstrom and Rosendhal (2006)**. There were significant differences in this arrangement compared to the FASTPOD Ropax design in

addition to the low speed range and larger unit size. As shown in Figure 8.6, firstly, the forward pods were fixed as wing pods whilst the steerable centre pods were located at the rear (opposite to the Ropax design). Secondly the steerable centre pods at the back were fitted with steering flaps for use at speed.

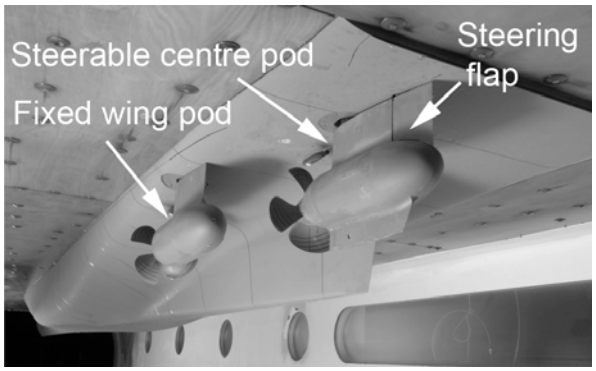

Figure 8.6: FASTPOD Container ship Pod arrangement, **Allenstrom and Rosendhal (2006)**

A complete ship model was tested to record cavitation behaviour of the pods (up to ±20°) as well as to measure the fluctuation hull pressures and propulsor acoustics. The intensity and cavitation extent on the suction side of the flap during the tests increased with increasing flap deflection angles being more aggressive for starboard side deflections. The study by **Allenstrom and Rosendhal (2006)** also drew attention to a large variation in the measured total pod unit (thrust) force with varying flap deflection angle, as shown in Figure 8.7.

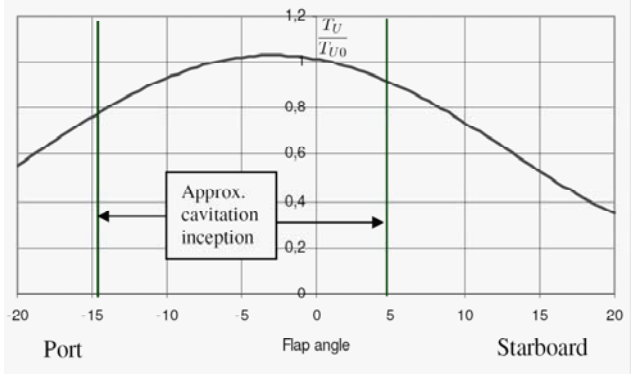

Figure 8.7: Effect of flap angle on the cavitation inception and unit thrust, **Allenstrom and Rosendhal (2006)**

The comparison of the pressure measurements at zero flap angles in atmospheric and design cavitation number indicated only 20% increase in the pressure due to cavitation that was judged to be less than normal.

In pursuit of manoeuvring loads for podded drive units**, Grygorowicz and Szantyr (2004)** compared the manoeuvring performance of a tanker driven by a single pusher pod to an equivalent twin puller pods counterpart. For the same pursuit **Heinke (2004)** drew attention on the significant change in the magnitude of forces and moments during manoeuvres at steering angles larger than ±10° and especially at crash stop by slewing the pod. Tests were conducted with a 4 and 5 bladed propeller fitted to a generic pod housing in pull and push mode over a full 360^0 azimuth. The variation of the force and moments on the pod unit and propeller were made together with comparisons of propeller and pod unit loads (pulling and pushing mode) relative to steering angle. The measurements made in the towing tank indicated that the loads are mostly irregular for the astern thrust conditions in the yawing angle range 90° to 270° due to separation at the propeller blades and pod housing. Since the propeller revolution can be reduced to zero during azimuth of the pod, a so-called "blocked propeller" test to include the effect of cavitation were conducted over a range of 360° at a constant velocity and different propeller revolutions including zero and at varying tunnel pressures including atmospheric.

In addition tests were conducted in dynamic condition of azimuth angles with constant turning rates in the angle range from 0° to 180° turning the pod inwards and outwards. It was found that the direction of azimuthing on the pod unit forces in blocked flow was remarkable while the rate of turn (from 30 to 40 °/s) resulted in rather small increase of the max forces and moments. Figure 8.8 shows a comparison of the forces and moments at a high advance coefficient (J = 2.62) at different steering angles for static and dynamic azimuth ranges. The comparison suggested that a quasi-static approach for predicting these loads can be acceptable for practical purposes. The effect of cavitation on the forces and moments

in the blocked propeller condition was found to be small and only small tip vortex cavitation was observed. The influence of the cavitation was also found to be small at large advanced coefficients.

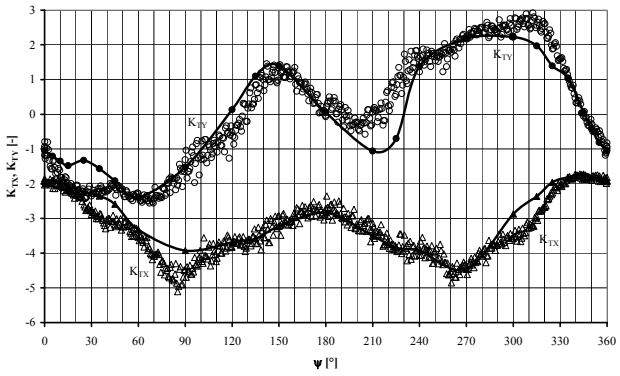

Figure 8.8: Comparison of propeller forces and moments at statically pod angles (continuous line) and dynamically controlled (scattered points) **Heinke (2004).**

In a PhD research **Stettler (2004)** and **Stettler et al. (2005)** presented a comprehensive analysis of the steady and unsteady dynamic manoeuvring forces associated with an azimuthing podded propulsor which was suitable for small-size underwater vehicles. A combined dynamic manoeuvring model for a surface vehicle with a DC motor driven azimuthing propulsor was proposed based upon standard nonlinear equations in the horizontal plane modified to account for the transient vectored forces by the propulsor plus the interaction terms. System identification and model parameters evaluation were achieved through a model test campaign performed on a notional pushing pod with a three-bladed fixed-pitch propeller which had a very large and flat faced hub that is relatively different to a conventional pod hub. Static and dynamic testing of the azimuthing propulsor were conducted using two test set-ups, the dynamically azimuthed propulsor system was tested first in isolation in a towing tank and second as part of an autonomous surface test vehicle on a PMM. A series of dynamic force tests and measurements were completed, and a series of wake visualisations using a new fluorescent paint method and PIV were completed to correlate the helical wake characteristics, velocities and forces for both static and dynamic propulsor states.

The load measurements in static condition indicated that the surge and sway forces showed a linear trend in the moderate range azimuthing angles (±45°) in a typical range of advance coefficients (J~0.36). Various peculiarities associated with small asymmetry due to pod housing and strut in front of the propeller as well as the rotational direction of the propeller were noted together with highly unsteady nature of the reversing wake in "crash-back" at larger steering angles greater than 90°. With the aid of wake flow visualisations some interesting force phenomenon in the quasi-static measurements were noted. Nearly constant helical wake pitch/diameter observations at varying azimuth angles were related to the trade off between the decreasing advance coefficient due oblique flow (cosine) effect and increasing induced axial velocity effect due to increased propeller loading. PIV measurements at 0 and 20 deg azimuth indicated that the average wake velocities for the 20° azimuth were considerably greater than the 0° condition that can be intuitively linked to an increase in thrust as measured in this condition (approx 20%). Furthermore the magnitude of the velocities measured at the upstream (outboard) side of the wake for the azimuthing case was higher than the downstream side enforcing the vortex wake into a distortion under the oblique inflow.

At the dynamic steering angles, the propulsor forces/moments due to the time rate of change in the propeller operating states were presented using step, ramp and sinusoidal control inputs. These allowed to identify the parameters of the non-linear model. Further supporting evidence from the wake flow visualisation were helpful to explain some transient load phenomenon that were caused by transient motions. In particular, the generation of a "vortex ring" due to a rapid change in the propeller rate was associated with the induction of an additional axial velocity at the propeller disc which reduces the angle of attack on the blades and hence thrust and torque. Similarly, the rapid transient changes

in the azimuth angles revealed the interesting phenomenon of sway force peak (or spike side force) which was also reported in **Woodward et al. (2005)** from slightly different perspective and the observed phase difference between this sway force peak and gradual progress (follow-up) of the blade wake was such that the propulsor force leading the azimuth angle of the propulsor as shown in Figure 8.9.

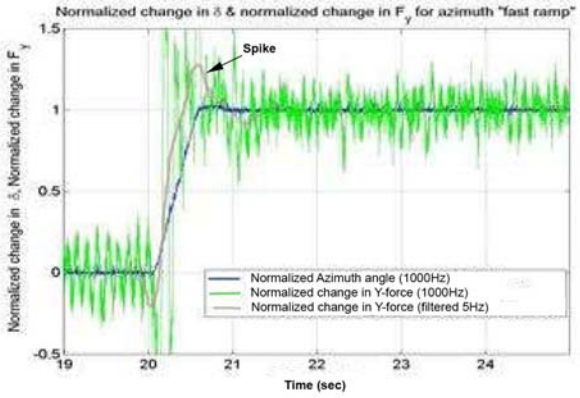

Figure 8.9: Sway force when pod undergoing a fast ramp change in azimuth angle from 0° to 60°, **Stettler et al. (2005)**

The most recent experimental investigation into the effect of steering angles on the podded propulsor loads was reported in **Islam et al. (2007a)** and **(2007b)**. The investigation involved systematic open water tests conducted with a puller and pusher type pod representative of in-service single screw podded propulsor. The results of the force measurements and moment calculations at static azimuthing were presented over a range of angles varying from 0° to ±30° and over a range advance coefficients. In both configurations the unit thrust coefficient decreased with increasing advance coefficient and for both azimuthing directions but in an asymmetric trend. The maximum unit efficiency for each configuration was reached at different steering angle and advance coefficient. In both configurations, positive azimuth angles showed an increasing transverse force with the increase of advance coefficient while the negative azimuth angles showed a decreasing transverse force. Also in both configurations zero transverse forces were found at all advance coefficients but in a slightly different range of angles on the port side. The pattern of the steering moment coefficients with varying azimuth angles and advance coefficients was completely different for each configuration.

In **Islam et al. (2007b)** the results of the force measurements and moment calculations during dynamic azimuthing were presented for the bollard pull and small advance coefficients. As a reference, according to SOLAS requirements, it was assumed that a full scale podded propulsor azimuths at a rate of 2.5°/s at vessel service speed, and approximately 5°/s during manoeuvring at slow speed. Depending on the ratio of the maximum vessel speed to the maximum steering torque at the lower speeds, a manoeuvring at 12°/s azimuthing rate was considered to be a special case. A first conclusion of this work was that load values measured under static azimuth angle are very close to mean values measured under dynamically azimuthing conditions. This finding confirms the results of a similar analysis **Heinke (2004)**. Nevertheless, interesting conclusions were derived by the analysis of time histories of forces and moments measured in dynamic conditions.

Time-dependant loads measurements revealed strong fluctuations due to the unsteady interaction between the propeller and the housing. For propeller as well as for the pod unit, the amplitude of dynamic load oscillations was comparable to the intensity of corresponding mean values. Load oscillations referred to mean values were higher at forward speed rather than at bollard pull, with peaks concentrated for particular values of the azimuthing angle which can be seen in Figure 8.10 where the unit longitudinal force peaks at about 150° azimuth angle.

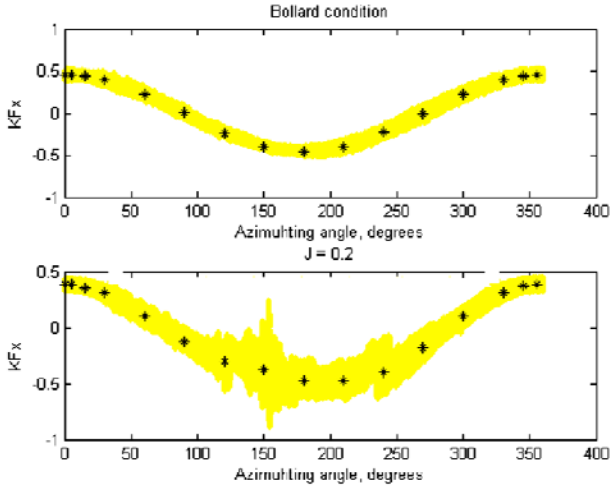

Figure 8.10: Longitudinal thrust coefficient on pod unit in static and dynamic azimuthing conditions, **Islam et al. (2007b)**

In order to evaluate hydrodynamic forces acting on the pod and propeller of ice going DAT tankers Tempera and Mastera, **Sasaki (2005)** conducted manoeuvring tests and pod unit open water test at a ±90° range of azimuth angles using scaled model of the actual pod system. From the results a simple prediction method was presented to predict propeller thrust and steering force of the pod system at steering conditions based on the idea of apparent propeller advanced speed J_δ by taking into account the displacement effect of the pod housing (i.e. $J_\delta = J_0 * \cos\delta + C * J_0 * |\delta|$, where C=0.35 and varies depending on the pod geometry) . The comparison of the prediction from this simple modelling and experiments is shown in Figure 8.11.

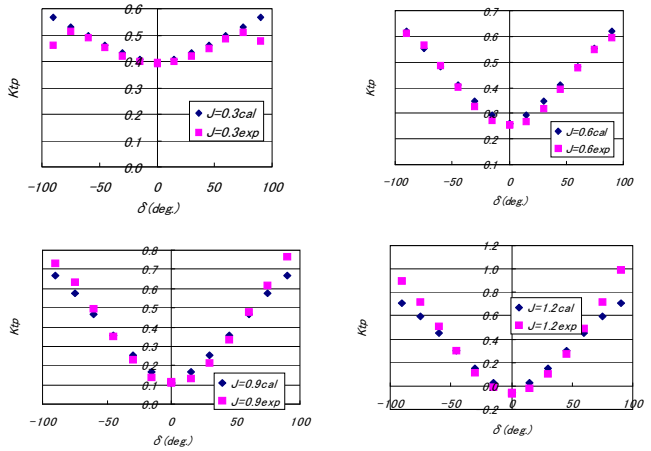

Figure 8.11: Comparison of predicted propeller thrust with experiments in steering conditions, **Sasaki (2005)**

8.3 Review of numerical investigations

There have been a variety of methods developed for numerical modelling of podded propulsors for performance prediction ranging from purely potential approaches to complete simulation of viscous flow. A good recent review of these methods was given by **Krasilnikov et al. (2006)** in presenting a viscous /potential coupled approach to study the propulsive characteristics of pulling and pushing podded propulsors under model and full scale conditions. In this study no emphasis was made on the effect of steering angle or cavitation although their approach appears to be applicable to model these effects.

Kinnas (2006) reported on the developments for performance prediction of various type propulsors including the podded drives. He gave a review of specific computational tools developed to predict unsteady cavitating flow around the propellers, which are based on vortex lattice or boundary element method (BEM) and to predict effective wake for the propeller, which is based on a finite volume method (FVM), by solving the 3D-Euler equations for the latter. An integral boundary layer solver to account for the effect of viscosity on the blades and on the pressure distribution over the blades has also been developed to correct the position of the cavity detachment and that of the leading edge vortex. These computational tools have been coupled in an iterative manner and applied to a podded propulsor to predict its basic performance. Further combination of the propeller solver with another computational tool, which is based on a boundary element method solving for the diffraction potential on the hull, enable to determine the unsteady hull pressure fluctuations. Although no example computations were given to demonstrate the effect of azimuthing angle on the podded propulsor performances the proposed hybrid approach and tools appeared to be able to tackle such predictions but requiring verifications and validations.

Deniset et al. (2004) also gave a good review of different CFD approaches to compute the flow around the whole podded propulsor and suggested to use another hybrid approach where a BEM for the propeller was coupled with a RANS for the entire pod housing in an iterative manner. In a follow-up study **Deniset et al. (2006)** discussed the practical difficulties of using RANS for the whole pod housing flow modelling and suggested to exclude the strut from the RANS computations but to include in the BEM computations. A comparison of the predictions for the time averaged pressure distributions along the strut chord of a puller pod showed excellent agreement with the measurements made by **He et al. (2006)**. Deniset et al. also included sample results for the strut lift coefficient at zero and 20° steering angle and reported on the ongoing development to couple this code with a sheet cavity model to be able to make complete analysis of a podded propulsor performance including the effect of cavitation.

As part of this committee's activities **Guo et al. (2007)** conducted a CFD analysis of the flow and loading around a puller type generic podded propulsor. The unsteady RANS simulations were conducted at 0°, 15°, 30° and 45° fixed azimuth angles at varying loading conditions. The simulation results were compared with the experimental results of a puller type podded propulsor model, which is shown in Figure 8.12, for the propeller thrust, torque and the lateral force of the pod unit obtained from the open water tests.

Figure 8.12: Model pod unit, **Guo et al. (2008)**

The comparison of the predicted open water performance data of the propulsor with the experimental data for the zero azimuth angle and over a range of advance coefficients indicated an underestimation varying between 0.8% to 6.5% for the propeller thrust coefficient (K_{T0}) and 4.7% to 6.8% for the torque coefficient (K_{Q0}), respectively.

Table 8.1 to 8.3 show the comparison of the CFD predictions with experiments for propeller thrust (K_T) and unit lateral force (K_L) as fractions of K_{T0} and propeller torque (K_Q) as a fraction of K_{Q0} for 15°, 30° and 45° azimuth angle, respectively. Both the numerical and experimental values of thrust and torque increase rapidly with increasing azimuth angle compared with those under straight ahead condition. The increase in loads reduces with increasing thrust loading coefficients. The correlation between the predicted and experimental values is better for the propeller thrust compared to the propeller torque and the unit lateral force which displays the worst correlation. The correlation also appears to deteriorate with increasing pod angles for the propeller thrust and torque while this is not valid for the lateral force.

Table 8.1: Comparison of computed and measured forces at helm angle of 15°

C_T		1	2	4	6	10
K_T/K_{T0}	Exp.	1.084	1.075	1.050	1.029	1.012
	CFD	1.109	1.079	1.055	1.038	1.022
K_Q/K_{Q0}	Exp.	1.155	1.128	1.075	1.040	1.020
	CFD	1.065	1.042	1.029	1.024	1.019
K_L/K_{T0}	Exp.	0.115	0.074	0.062	0.050	0.020
	CFD	0.180	0.122	0.078	0.061	0.045

Table 8.2: Comparison of computed and measured forces at helm angle of 30°

C_T		0.94	1.18	2.33
K_T/K_{T0}	Exp.	1.431	1.391	1.230
	CFD	1.342	1.283	1.164
K_Q/K_{Q0}	Exp.	1.405	1.383	1.285
	CFD	1.238	1.199	1.114
K_L/K_{T0}	Exp.	0.243	0.224	0.143
	CFD	0.406	0.326	0.206

Table 8.3: Comparison of computed and measured forces at helm angle of 45°

Finally Figure 8.13 shows the flow pattern around the propulsor at 45° azimuth angle for further information.

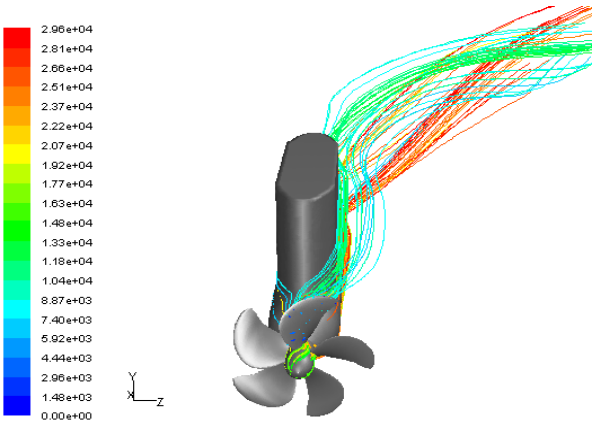

Figure 8.13: Flow pattern around podded propulsor at 45° pod steering angle, **Guo et al. (2008)**

8.4 Concluding remarks

Complex interaction between the propeller and pod housing in wide range steering conditions has been explored mainly experimental and in model basins while the tests in cavitation tunnels have mainly concentrated on the optimisation of pod unit orientation limited to small and fixed pod toe-in/out angles.

Limited model tests and full scale observations have revealed no serious cavitation concerns typical podded propulsors for normal steering angles beyond which thickening tip vortices combined with spreading blade sheet cavitation, which can be unsteady, will become a concern. Depending on the steering angle, cavitation may also develop typically on the strut leading edge, pod tail end and bottom fin if the latter exists. Fluctuating hull pressures are sensitive to the steering angle and can grow in magnitude significantly beyond typically 3°-4° of steering angle.

C_T		0.94	1.18	2.33
K_T/K_{T0}	Exp.	1.812	1.765	1.556
	CFD	1.761	1.601	1.346
K_Q/K_{Q0}	Exp.	1.711	1.665	1.463
	CFD	1.465	1.424	1.252
K_L/K_{T0}	Exp.	0.403	0.366	0.211
	CFD	0.567	0.455	0.298

For podded propulsors on high-speed vessels, cavitation and its sensitivity to steering angles become rather serious even at smaller values requiring special attention and hence consideration of carefully controlled flaps for steering.

Time-dependent propulsor loads recorded in dynamic conditions can display strong fluctuations requiring further investigations. Also the effect of cavitation in these conditions requires further quantification and hence investigation.

Although RANS based CFD methods have made significant progress to predict the podded propulsor loads under the effect of steering, their applications -including the effect of cavitation- are not practically feasible. Currently, hybrid CFD tools appear to be a better choice to tackle this task but require comprehensive validation..

9. SPECIAL PPLICATIONS FOR PODDED PROPULSION

9.1 Introduction

This section presents a brief update on the special applications of podded propulsors since the 24th ITTC reporting.

9.2 Ice Applications

Icebreaker design and operation changed radically with the introduction of the Double Acting Ship (DAS) concept. The 16MW Azipod driven vessels Tempera and Mastera introduced in 2002-2003 reported by **Sasaki et al. (2004)** exceeded their expectations and won international recognition for their innovative yet simple design approach.

Development of the double acting concept continue to be made; the US Coast Guard took delivery in 2005 of the 6.8MW USCG Makinaw **(USCG (2008))** the first podded vessel in their fleet, as did the Norwegian Coast

Guard with MS Svalbard. Aker Yards (formerly Kvaerner Massa-Yards) also extended their portfolio in 2006 with the launch of the 13MW M/V Norilskiy Nikel, a DAS container ship. The ship was fitted with a heavily cutaway icebreaking bow of approximately the same form as the SA-15 class whilst the DAS tankers Tempera and Mastera have bows optimized for open-water navigation, one of the general ideas of the double-acting principle. The ship was instrumented at the construction phase to measure ice loads and Ice trials have already taken place, the results have been summarised by **Hanninen et al. (2007)**. Clear safety margin between class rule design loads and actual operational loads was observed. **Wilkman et al. (2007)** also reported on sea trials of Norilskiy Nickel illustrating a sample of the results for ahead and astern conditions at 13MW.

The latest vessels to use DAS technology are a pair of 70,000dwt Arctic shuttle tanker projects (twin 8.5MW Azipod) underway at Admiralty shipyards in Russia and Samsung Heavy Industries yard in Korea; both projects are for Sovkomflot. Three further 70,000dwt tankers again from an Aker Arctic / Samsung partnership for Sovkomflot given by **Niini et al. (2007)** will be delivered sequentially in 2007, 2008 and 2009.

Beyond the double acting concept other authors such as **Park et al. (2007)** have presented results of development of ice breaking tanker series with different bow concepts. The performance of three bow shapes such as extreme, moderate ice breaking bow and conventional ice strengthened bow were evaluated by the model tests in ice basin (AARC) and towing tank (SSMB) to find the best fuel economy including ice capability in Arctic and Baltic Sea.

Molyneux & Kim (2007) described the methods of model testing in ice that have been developed at the Institute for Ocean Technology (IOT), Canada, over the last decades and applied and refined under collaborative project with SHI for predicting the performance of large tankers in ice. Experimental results on four hull designs with different propulsion arrangement have led to suggestions for refining the modelling techniques for future projects. In particular further study of the concept of pre-sawn ice resistance experiment is required for unconventional icebreaking hull forms with bulbous bow. Besides, a typical scale for a tanker model at IOT is approximately 1:35 while full scale-model correlation data are available for 1:22 icebreakers typical scale. Since the material structure of model ice does vary with ice thickness and this may have some effect on the most appropriate value of the hull-ice friction coefficient, obtaining full scale trial data from an oil tanker may become key element of the last evaluation.

Ice-going LNG carriers with pod propulsors were already on the drawing board in the mid 1990's when LNG carriers were built in Finland. **Ishimaru et al. (2007)** discussed the practical design of LNG Carriers from shipbuilder's point of view including the selection of the propulsion system. **Suojanen (2007)** discussed the development of the technical design of large size arctic LNG Carrier including various versions and solutions for icebreaking operation.

Development of relevant requirements becomes imperative in view of the tendencies of the modern active ice-going fleet progress. **Andryushin (2007)** introduced main results of research dedicated to the development of new requirements of RS for icebreaking propellers (IP) and propulsion complex (PC) covering double-acting icebreaking vessels. Given in the paper conclusions from prior operating experience indicates that IP blade scantlings are generally to be assigned such us to ensure not only static strength but fatigue as well. Key points of such approach with reference to the same in draft of RS requirements are presented. The method to assign the blade damage force under action of spindle torque and bending moment has been developed. This method was taken as a normative one and implemented into draft of RS requirements. The method has been developed for ensuring the strength of the propulsion complex components at elastoplastic deformation in stress concentration areas. As the main outcome of

development of the requirements for propulsion complex, pyramidal strength has been stated. Within a scope of special consideration the draft of RS requirements have been used for designing and approval of technical documentation for the PC of modern ice-going vessels and icebreakers, including double-acting ships.

Building and entry into service of new ships, continuing development of DAS concept, emphasizes actuality to investigate different aspects of DAS design and exploitation. In particular it may refer to the effect of ice blockage on propeller. Omission of cavitation effects in podded propulsion ice test procedures has been highlighted by **Atlar & Sampson (2005)** in written comments to the 24th ITTC Specialist Committee on Ice with reference to on-going research. By now **Sampson, et al. (2006b)** have presented results of systematic study of the effect of cavitation during propulsor ice interaction in Emerson Cavitation Tunnel. At the first stage the blockage tests of actual DAT propulsor model were entirely static and considered simulated ice blocks positioned at fixed distances from the propeller. Large matrix of data over a wide range of parameters has been generated by variation of simulated ice block itself (simulating range of depth of cut and depth of recess), tunnel speeds and vacuum conditions. Propeller thrust, torque, pressure pulse and noise have been recorded as well as visual observation has been recorded by digital video and photography. Evident in all of the figures presented in the papers was developed sheet cavitation on the blade section obscured by the shadow of the blockage, together with bursting tip vortex cavitation in the blockage wake. Significant impact of cavitation on the performance of an ice class propeller has been observed in general and these findings have been attributed to the actual DAT propulsor operation conditions with certain limitations. Besides, the blade loading show dramatic oscillations about the mean load during blockage as shown in Figure 9.1.

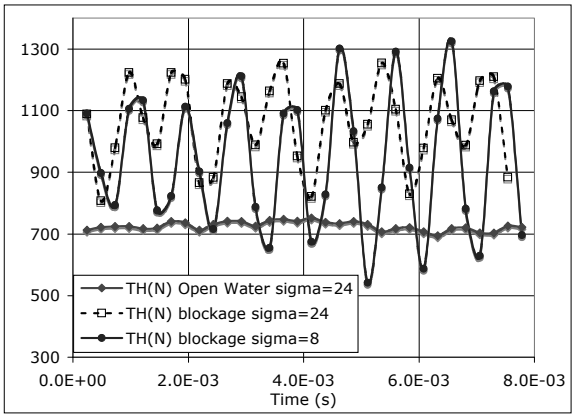

Figure 9.1: Loading comparison **Sampson, et al. (2006b)**

The observed cavitation was violent and highly erosive nature. The tests also showed the cavitation generated elevated level of noise. It has been concluded that cavitation is dominant in the blockage test. Further results with ice milling simulation using crushable foam have been introduced by **Sampson et al. (2007a, 2007b)** with test matrix covered the same range of parameters as the blockage test.

9.3 CRP Podded Propulsion Systems

The advent of a podded propulsor with multi component propellers is a logical development of electric propulsion in marine vehicles. Pure CRP pods, the so-call hybrid CRP system and pump jet pod (PJP) are typical applications of energy saving concepts applied to existing podded propulsion systems. However, the current experimental techniques and procedures for such multi-component podded propulsors are not sufficient for such demands.

The hybrid CRP system is expected to be a major application for the concept of pod propulsor unit and contra-rotating propeller. The combined high efficiency of CRP and the excellent maneuverability of podded propulsors make the hybrid CRP system extremely attractive. Two RoPax ferry has been already built and now under the commercial operation reported by **Ueda et al. (2004)**. However the hybrid CRP is difficult to be tested by routine test procedures used for conventional ships with single screw propeller or with single podded propulsor. Moreover, the extrapolation method to the full-scale

performance prediction has not been fully established due to the uncertainty in the analysis of full-scale resistance of pod housing. In these difficult backgrounds, some detailed experiments were made and the experimental results have published in papers such as **Allenstrom & Rosendahl (2006)** and **Pêgo et al. (2007)**. These excellent results shed light upon the flow field of the hybrid CRP propulsor.

In Japan, an innovative podded propulsor ship, named "Shige Maru" was launched at Niigata Shipbuilding & Repair Corp. (NSR) in October 2007 (DNV "tanker"). She is a domestic coast tanker of 4999GT and has two sets of podded drive with contra-rotating propeller each of which absorbs 1250 kW shown in Figure 9.2.

Figure 9.2: Pure CRP pods on the Shiga Maru

Shige Maru is one of the ships delivered as "Super EcoShip". The Super EcoShip project was led by Ministry of Land, Infrastructure and Transport and National Maritime Research Institute from 2001. The project has ended its R&D term in 2005, and now in the phase of practical application with the aid of JRTT and NEDO, both of which are governmental organizations.

9.4 Rim driven podded propulsor

Rim-Driven Podded propulsor (RDP) was developed and patented by the General Dynamics Electric Boat (EB) Corporation during the first half of 2000. The RDP propulsor integrates a ducted multiple blade row propulsor with a permanent magnet, a radial flux rotor mounted on the tips of the propulsor rotor blades and a stator mounted within the duct. The stator is located behind the rotor and faces the incoming flow in a tractor pod configuration, **Van Blarcom et al. (2002).** The claimed advantages compared to a conventional Hub Driven Pod (HDP) include: smaller geometrical size at 1/3 length of an equivalent power HDP; relatively higher efficiency; dramatic reduction in hull pressure at 1/5 magnitude of an equivalent HDP pressures; reduced performance degradation in off-design conditions; higher speed capability with a reduced risk of cavitation and no risk of erosion and more flexibility in installation at the aft end due to smaller size. In a later study **Van Blarcom et al. (2004)** reported that a 1.6MW RDP demonstrator completed in air testing and plans were drawn for at-sea testing in 2006. The recent update on the Office of Naval Research Advanced Electric Ship Demonstrator (AESD), which is a 40.5m long and 120 tons test platform, indicates that the EB's RDP with a control system provided by Rolls Royce will be tested on this demonstrator and called "Rimjet" propulsor, **ONR (2008),**

9.5 Hybrid pod and waterjet propulsor

By considering potential limitations, which can be imposed by the pod at high speeds, there could be an attractive hybrid propulsion solution where a pod propulsor is combined with a water-jet to take the advantage of a higher propulsive efficiency of the waterjet at high speeds as well as the flexibility of a hybrid system. Such propulsion system was explored on a Ropax ship in a collaborative effort within two recently completed EU projects, VRSHIPS-Ropax and FASTPOD as reported by **Atlar et al. (2006).** The hybrid system is composed of two steerable (wing) pod drives and two fixed (central) – booster – flush type water jets as shown in Figure 9.3 in model scale. In these projects a similar Ropax hull with different size were explored. Therefore, based upon the FASTPOD Ropax steer-able pod design but with a smaller propeller diameter and the same power absorption of 27MW per pod, a new set of propeller was designed, and tested on the VRSHIPS-Ropax hull. **Koiker et al. (2005)** reported a trial speed of 37.4 knots was confirmed in the propulsion

tests for a total shaft power of (2 × 27MW + 2 × 27MW = 122MW), which was equally distributed amongst the 2 pods and 2 waterjet units, at a propeller rate of 179 rpm.

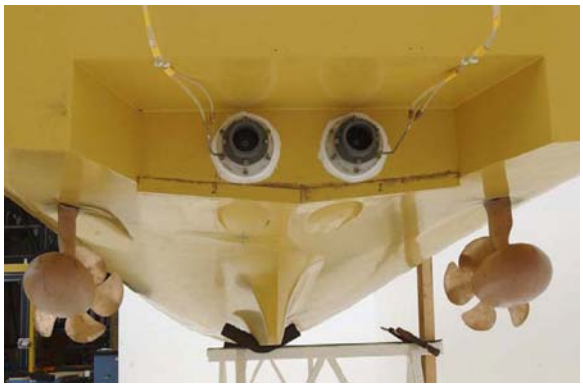

Figure 9.3: Combined pod and waterjet setup, **Atlar et al. (2006).**

As reported by **Johannsen and Koop (2006) c**avitation tunnel tests with the VRSHIPS-Ropax hull at the trial condition displayed more extensive but stable sheet cavitation. However, the hull pressure measurements in this condition were much higher with a maximum value of 7.6 kPa; more than twice the pressure values induced by the FASTPOD steerable pod unit. It was suggested that a comfortable level of 3.5 kPa could be reached by transferring 5MW/unit from the pod drives to the waterjet units.

9.6 Pump jet pod

Through a joint reserach effort during 2005-2006 led by ALSTOM (Chantiers de l'Atlantique) and conducted by Bassin des Carenes (BEC) and DCNS a new generation pusher type of ducted pod which is entitled "Pump Jet Pod" (PJP) was reported by **Bellevre et al. (2006).**

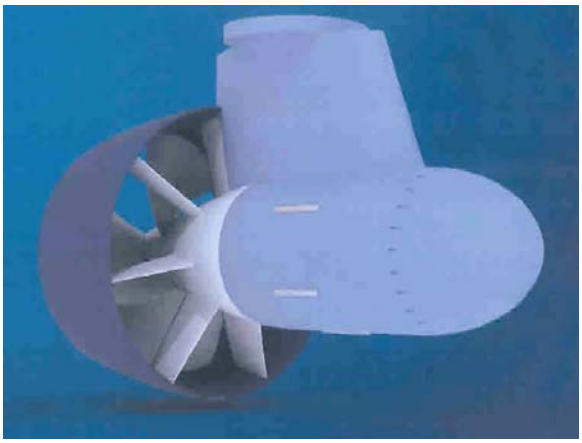

Figure 9.4: Pump jet pod (PJP) unit

The PJP is a hub driven pusher pod as shown in Figure 9.4. The unit has multi-row stator blades situated in front of the rotor that are supported by the hub and duct/nozzle, which fully covers the rotor and stator. An elongated azimuthing pod housing combined with a strut at the front also supports the assembly of the rotor, stator and duct.

A comprehensive numerical and experimental design study was conducted for 2 cruise liner type pod units (13MW) for a 45000 GRT cruise liner using 2D-3D RANS codes. Based upon this comparative study it was concluded that the propulsive performance of PJP was 14% higher than the conventional tractor pod mainly due to its superior open water efficiency. Pressure pulses with the PJP were also 80% lower; no cavitation was experienced at the design condition. The slewing torque of PJP was approximately 30 times smaller than the tractor pod in addition to being in a stable equilibrium. Furthermore considerably smaller size and compact design of PJP provided an additional advantage of flexible aft end design and better interaction of PJP with the hull.

9.7 Concluding remarks

The pod application for ice-going ships is expected to be comparable to that of the wide application seen for cruise liners.

Results from the published R&D projects into podded drives demonstrate the attraction of special pod applications such as CRP pod concept in terms of expected efficiency and good manoeuvrability. Hybrid CRP systems

based on the concept of pod propulsor unit and contra rotating propeller are expected to be more widely adopted.

Investigation on Pump Jet Pod (PJP) reveals this propulsor to be the latest development of innovative pod applications. Among expected advantages of the PJP are its compactness, efficiency and reduced pressure pulses.

Use of pod drives in combination with water jet propulsors looks attractive for fast ships demonstrating higher propulsive efficiency and less erosive cavitation in spite of some disadvantages attributed to higher pressure pulses which can be overcome by distribution of the loading.

Experimental techniques and procedures, including extrapolation to the full scale performance prediction and cavitation behaviour have not been fully established for these special pod applications. Some detailed experiments were already made however concentrated research work is expected to establish reliable and accurate experimental procedures for above mentioned pod propulsors.

10. TECHNICAL CONCLUSIONS

(1) Procedure of pod tests and extrapolation are established however, full scale data to evaluate this method will be needed.

(2) A lot of complex system of pod propulsion such as CRP type and a hybrid type has appeared and they are not deeply studied so far because of lack of full scale data of such kinds of pod systems.

(3) A pod performance at off design condition or maneuvering condition is so important to affect on not only cavutation and vbration but also fuel consumption. Tjere are many papers mentioned above cavitation and vibrations at pod steering conditions however, it is also important to design the pod from propulsive performance view point taking an efficiency loss at smaller helm angle (less than 10deg.).

(4) CFD becaomes very strong tool now to evaluater the scale effect of pod housing drag and extrapolation method.

11. REFERENCES

Allenstrom, B. and Rosendhal, T., "Experience From Testing of Pod Units in SSPA's Large Cavitation Tunnel", 2nd T-POD Conference, Session 5, 3-5 October, University of Brest, France.

Andryushin,A.V. (2007), "Modern RS Requirements and Methods Ensuring Operating Strength of Icebreaking Propulsion Complex", Proc.of International Conference on Design and Construction of Vessel Operating in Low Temperature Environments, London, UK

Atlar, M., Clarke, D., Glover, E.J., McLean, D., Sampson, R. and Woodward, M.D. (Editors), (2004), "T-POD, 1st Intl. Conference on Technological Advances in Podded Propulsion", Proceedings, University of Newcastle, 14-16 April, UK, p 547.

Atlar, M., Sampson,R., (2005), "Written Comments to the 24th ITTC Specialist Committee on Ice", International Towing Tank Conference,Edinburgh,Scotland.

Atlar M., Woodward, M.D., Besnier, F., Rosendhal, T., Konieczny, L. and Depascale, R., (2006) "FASTPOD Project: An Overall Summary and Conclusions", Opening Session, Proc. of 2nd T-POD Conference, Brest, France.

Bellevre D., Copeaux P. and Gaudin C., (2006) "The Pump Jet POD An Ideal Means to Propel Large Military and Merchant Ships", Proc. of 2nd T-POD conference, Brest, France

Billard, J.Y., Atlar, M. and Laine, C., (Editors), (2006). "T-POD 2006, The 2nd Intl.

Conference on the Technological Advances in Podded Propulsion", [online], http://tpod06.ecole-navale.fr

Bretschneider, H. and Koop, K.-H., 2005,"Cavitation Tests with Design Propellers for the FASTPOD Ropax Vessel", HSVA Report, K 17/04.

Chicherin, I.A., Lobatchev, M.P., Pustoshny, A.V. and Sanchez-Caja, A., 2004, "On a Propulsion Prediction Procedure for Ships with Podded Propulsors using RANS-Code Analysis" 1st T-POD, University of Newcastle, UK, p. 223-236.

Converteam, (2007), [online] www.converteam.com/converteam/1/doc/News/20070903_Converteam_DCNS_Inovelis_B.pdf

Deniset, F., Billard, J.-Y. and Jouen, R., "Fluctuating Pressure Distribution on a Pod", 1st T-POD Conference, 14-16 April, University of Newcastle, UK, p. 237-244.

Deniset, F., Laurens, J.-M. and Romon, S., 2006, "Computation of the fluctuation pressure Distribution on the Pod Strut", 2nd T-POD Conference, Session 7, 3-5 October, University of Brest, France.

Eaton, J.E. and Billet, M.L., 2004, "Pod Propulsion Research and development at ARL-Penn State", T-POD, 14-16 April, University of Newcastle, UK, p. 89-106

Felli, M., Monti M. and Poisson, F. and Guj, G., (2006) " Experimental Analysis of the Podded Propeller Rudder Interaction", Session 8, Proc. of 2nd T-POD Conference, University of Brest, France

Funeno, I.: "Hydrodynamic Development and Propeller Design Method of Azimuthing Podded Propulsion System", 9th Symposium on Practical Design of Ships and Other Floating Structures (PRADS2004) , Volume 2, pp.888-893(2004)

Friesch, J., 2004, "Cavitation and Vibration Investigations For Podded Drives", T-POD, 14-16 April, University of Newcastle, UK, p. 387-399.

Greco, L., Colombo, C., Salvatore, F. and Felli, M., (2006) "An Unsteady Inviscid Flow Model to Study Podded Propuslor Hydrodynamics", Session 8, Proc. of 2nd T-POD Conference, University of Brest, France

Grygorowicz, M., Szantyr, J.A., 2004 "Open Water Experiments with Two Pod Propulsor Models", T-POD, 14-16 April, University of Newcastle, UK, p. 357-370

Guo, C-Y,Yang, C-J and Ma, N., 2008, "CFD Simulation For a Puller Type Podded Propulsor Operating at Helm Angles", Private Communications with the 25th ITTC Specialist Committee for Azimuthing Podded Propulsion.

Hoerner, S.F., 1967 Fluid Dynamic Drag

Holtrop, J., 2001, "Extrapolation of Propulsion Tests for Ships with Appendages and Complex Propulsors", Marine Technology, 38 (3), p.145-157

Hanninen, S.,Ojanen, M.,Uuskallio, A. & Vuorio, J., (2007) ,"Recent development of Podded Propulsion in Arctic Shipping", Proc. of POAC-07 Intl. Conference, Dalian,China

He M., Veitch B., Bose N., Bruce C. and Liu P., 2006, "Numerical Simulations of a Propeller Wake Impacting on a Strut", CFD Journal, Vol. 15, No 1, April, p. 79-85.

Heinke, H.J., 2004, "Investigation about the Forces and Moments at Podded Drives", T-POD, 14-16 April, University of Newcastle, UK, p. 305-320

HTA, (2006), "HYDROTESTING ALLIANCE – Network of Excellence", [online], http://hta-noe.eu

Ishimaru, J. ,Tsumura, K., Sato,K., Ishida,T., & Oka, M., (2007) ,"Practical Design of LNG

Carriers in Low Temperature Environments", Proceedings .of International Conference on Design and Construction of Vessel Operating in Low Temperature Environments, London, UK

Islam, M.F., Veitch, B. and Liu, P. (2007), "Experimental Research on Marine Podded Propulsors", Proceedings, 7th International Conference on Mechanical Engineering ICME-ABS-167, Dhaka, Dec. 30-31, 7 p.

Islam, M.F., Veitch, B., Akinturk, A., Bose, N. and Liu, P., 2007a, "Experiments with Podded Propuslors in Static Azimuthing Conditions". 8th CMHSC, St John's, NL, Canada

Islam, M.F., Veitch, B., Akinturk, A., Bose, N. and Liu, P., 2007b, "Performance characteristics of a Podded Propulsor During Dynamics Azimthing", 8th CMHSC, St John's, Canada

ITTC, 1999, "The Specialist Committee on Unconventional Propulsors, Final Report and Recommendations to the 22nd ITTC", Proceedings of the 22nd ITTC, Seul-Shanghai, Vol 2, p. 311-344

ITTC, 2002b, "Open Water Test", 23rd International Towing Tank Conference, Venice, ITTC Recommended Procedures, Procedure 7.5-02-03-02.1, Rev 01, p. 1-9

ITTC, 2005, "The Specialist Committee on Azimthing Podded Propulsion, Final Report and Recommendations to the 24th ITTC", 24th ITTC, Edinburgh, Vol 2, p. 543-600.

Johannsen, C. and Koop K-H., 2006, "Cavitation Tests for Two Fast Ferries with Pod-Drives Carried out in HSVA's Large Cavitation Tunnel HYKAT", 2nd T-POD Conference, Session 5, 3-5 October, University of Brest, France.

Kano, T., Kayano, J., Sakoda, M. and Takekuma, K., "Manoeuvrability of 749GT Cement Tanker with Three Different Pod Propulsion Systems", Session 1, Proc. of 2nd T-POD Conference, University of Brest, France

Kinnas, S.A., 2006, "Prediction of Performance and Design of Propulsors – Recent Advances and Applications", 2nd T-POD Conference, Opening Session, 3-5 October, University of Brest, France.

Kooiker, K., Verhulst, M and Kerkhof, R., (2005), "Calm water model tests for a fast Ropax vessel with hybrdi propulsion system – Task 9.5 of the VRS Ropax Project", MARIN report 15643-1-DT/VT, October.

Krasilnikov, V., Ponkratov, D., Achkinadze, A. and Jia Ying, S., 2006, "Possibilities of a Viscous/Potential Coupled Method to Study Scale Effects on Open-Water Characteristics of Podded Propulsors, 2nd T-POD Conference, Session 7, 3-5 October, University of Brest, France.

Lea, M., Thompson, D., Van Blarcom, B., Eaton, J., Richards, J., and Friesch, J., 2002, "Scale Model Testing of a Commercial Rim-Driven Propulsor Pod", SNAME Annual Meeting

Lobatchev, M.P., Chicherine, I.A., 2001, "The Full Scale Estimation for Podded Propulsion System by RANS Method" Lavrentiev Lectures, St. Petersburg, Russia, 19-21 June, p. 39-44

Mewis, F., 2001, "The Efficiency of Pod Propulsion", HADMAR'2001, Bulgaria, Vol 3

Mistral (2006), "BPCMistral", [online], http://bpcmistral.free.fr/

Molyneux, D. & Kim, H.S. (2007) "Model Experiments to Support the Design of Large Icebreaking Tankers", Proc.of Int. Conference on Design and Construction of Vessel Operating in Low Temperature Environments, London, UK

Niini, M., Kaganov, S. & Tustin, R. (2007). 'Development of arctic double acting

shuttle tankers for the pirazlomnoye project. In TSCF 2007 Shipbuilders Meeting .

ONR, (2008), "ONR's Advanced Electric Ship Demonstrator Will Test Revolutionary Rimjet Propulsion System" [online], ww.onr.navy.mil/media/

Oosterhuis, G. (2006), "Model-Scale Podded Propellers For Maritime Research", PhD Thesis, University of Eindhoven.

Park, H.G., Jung, H.C.,Lee, Y.C., Ahn, S.M. and Hwangbo, S.M., (2007) "A Study on Hull Form Development for Ice Breaking Vessel in the Arctic", Proc. of POAC-07, Dalian, China

Pêgo, J. P., Lienhart H. & Durst F. (2007) "Mean velocity and moments of turbulent velocity fluctuations in the wake of a model ship propulsor", Experiments in Fluids Springer Berlin / Heidelberg, Volume 43, Numbers 2-3, 2007

Pustoshny, A. V. and Kaprantsev, S. V., 2001, "Azipod propeller blade cavitation observations during ship manoeuvring", 4th Int. Symposium on Cavitation (CAV'2001), Pasadena, USA

Sampson, R., Atlar, M. & Sasaki, N., (2006). "Propulsor Ice Interaction - Does Cavitation Matter?", CAV 2006, Wageningen, The Netherlands.

Sampson, R., Atlar, M. & Sasaki, N. (2006) "Ice Blockage Tests with DAT Tanker Podded Propulsor", Proc. of 2nd T-POD conference, Brest, France

Sampson, R., Atlar, M. & Sasaki, N. (2007) "Effect of Cavitation During Systematic Ice Block Tests", Proceedings of POAC-07 Dalian, China

Sampson, R., Atlar, M. & Sasaki, N., (2007), "Ice Blockage Tests with a Podded Propulsor - Effect of Recess. " Proceedings of 27th International Conference on Offshore Mechanics and Arctic Engineering.

Sánchez-Caja, A., Ory, E., Salminen, E., Pylkkänen, J. and Siikonen, T., 2003, "Simulation of Incompressible Viscous Flow Around a Tractor Thruster in Model and Full Scale". The 8th International Conference on Numerical Ship Hydrodynamics, 22-25 September, Busan, Korea

Sasaki, N., Laapio, J., Fargerstrom, B. and Juurmaa, K., 2002, "Model Tests of Ice Going Acting Aframax Tanker", Proc. of 7th Canadian Marine Hydrodynamics and Structure Conference, Vancouver, Canada

Sasaki, N., Laapio, J., Fagerstrom, B., Juurmaa, K. & Wilkman, G. (2004). "Full scale performance of tankers Tempera and Mastera. " First International conference on Technological Advances in Podded Propulsion (T-POD), Newcastle upon Tyne.

Sasaki. N. (2005) "Chapter 7 Podded Propulsion System" JTTC 5th Propeller symposium, Tokyo,Japan

Stettler, J.W., 2004, "Steady and Unsteady Dynamics of an Azimuthing Podded Propulsor Related to Vehicle Maneuvring", PhD Dissertation, Massachusetts Institute of Technology.

Stettler, J.W., Hover, F.S., and Triantafyllou, M.S., 2005, "Investigating the Steady and Unsteady Maneuvering Dynamics of an Azimuthing Podded Propulsor", Trans. SNAME, p. 122-148

Suojanen, R. (2007) "Technical Development of LNG Carriers for Harsh Ice Conditions", Proceedings of International Conference on Design and Construction of Vessel Operating in Low Temperature Environments, London, UK

Szantyr, J.A., 2001a, "Hydrodynamic Model Experiments with Pod Propulsor", International Symposium of Ship

Propulsion (Lavrentiev Lectures), State Marine Technical University, St. Petersburg, Russia, p. 95-104

Trägårdh,P, Lindell, P, Sasaki, N.(2004) "DOUBLE ACTING TANKER – Experiences from model tests and sea trials. First International conference on Technological Advances in Podded Propulsion (T-POD), Newcastle upon Tyne.

Ueda, N., Oshima, A., Unseki, T., Fujita, S., Takeda, S. and Kitamura, T., (2004) "The First Hybrid CRP-POD Driven Fast ROPAX Ferry in the World", Mitsubishi Heavy Industries Ltd, Technical Review, Vol. 41, No. 6, p. 1-4.

USCG, (2008), "GLIB–mackinaw", [online], www.uscg.mil/d9/cgcMackinaw/

Van Blarcom, W., Hanhinen, J. and Mewis, F., 2002, "The Commercial Rim-Driven Permanent Magnet Motor Propulsor Pod" SNAME Annual Meeting, September

Van Blarcom, B., Franco, A., Lea, M., Peil, S. and Van Dine, P., 2004, "Rim-Drive Propulsion-Improving Reliability and Maintainability Over Today's Pods", T-POD, 14-16 April, University of Newcastle, UK, p. 73-88

VRSHIPS-Ropax, (2000), "Life-Cycle Virtual Reality Ship System(s), Annex-1, Description of Work", European Comission RTD FP5 Project, GRD1-2000-25709, University of Strathclyde (co-ordinator)

Wang, D., Atlar, M. and Paterson, I., 2003, "Cavitation Observations, Hull Pressures and Noise Measurements with the OPTIPOD Supply Ship in Cavitation Tunnel", Newcastle University Report, MT-2003-003.

Wilkman, G., Elo, M., Lonnberg, L. and Kunnary, J., (2007) "Ice trials of MV Norilsky Nickel in March 2006", Proc. of POAC-07 Dalian China

Woodward, M.D., Atlar, M. and Clarke, D., 2005b, "Manoeuvring induced loads on fast pod drives", FAST'2005, 27-30 June, St. Petersburg, Russia, 8 p

Van Rijsbergen, M. and Holtrop, J., 2004, "Investigations on a pod open water test set-up", MARIN Internal Report, No: 16115-1-DT

Veikonheimo, T., 2006, "Private communications", ABB Oy, Marine & Turbocharging